UNIVERSITY OF GENOA

DEPARTMENT OF EXPERIMENTAL MEDICINE

PhD COURSE IN EXPERIMENTAL MEDICINE

Curriculum: *Molecular and Cellular pathology of age-related diseases*

Role of PKC-α in the induction of ferroptosis: a therapeutic target to fight chemoresistance of cancer stem cells

Candidate

Lorenzo Monteleone

Tutor

Prof. Cinzia Maria Domenicotti

PhD Coordinator

Prof. Ernesto Fedele

Academic Year 2020-2021

XXXIV Cycle

Table of contents

List of figures

Introduction

Tumor is a mass of cells that grow in an afinalistic and progressive way and acquire a typic morphological and functional characteristics in respect to healthy cells. According to growth and behavior, tumors can be divided into benign and malignant: the first ones have local expansive growth and do not spread; the second ones grow invasively, spread by forming metastases, induce cachexia (a condition of generalized atrophy) and may, potentially, lead to patient's death.

Cancer is considered an age-related disease (Fig. 1): more than 50% of cancers occurs in people over 70 years (Berger N.A. et al., 2006; Siegel R.L. et al., 2015). In fact, by considering that the life expectancy is now exceeding 80 years, the World Health Organization (WHO) has extimated that in the next years cancer will affect an increasing number of people with a higher incidence in the older subjects.

Several factors can explain the association between cancer and aging (Fig. 1). Firstly, the life-long exposure to exogenous factors (such as UV irradiation and environmental agents) and endogenous metabolic products (such as free radical species) that induce the accumulation of oxidative stress-induced DNA mutations with irreversible cell damageand impact on the total body (Yin D., 2015). Secondly, aging leads to an accumulation of senescent cells which, by secreting inflammatory mediators (such as IL-6, IL-8), give rise to a microenvironment able to sustain tumor growth (Finkel T. et al., 2007; McHugh D. et al., 2017).

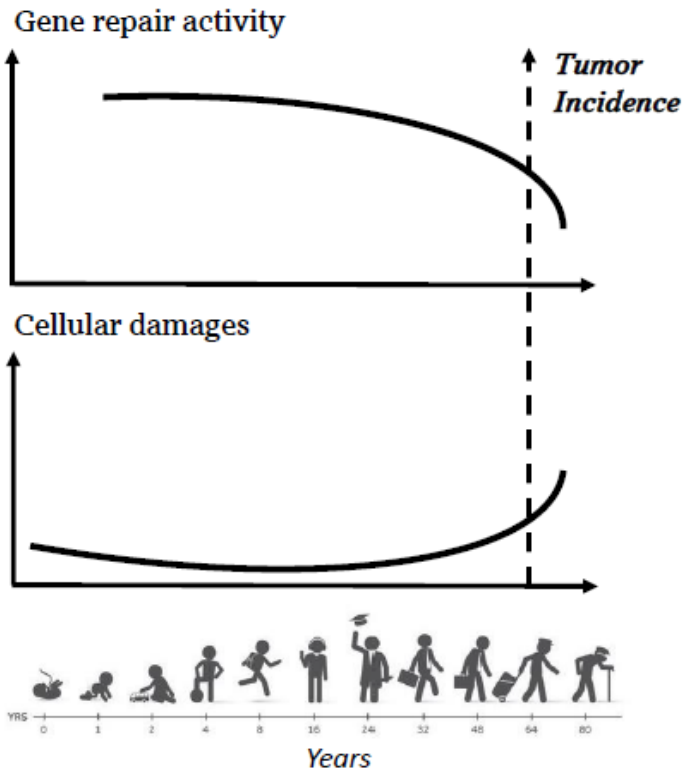

Figure 1. Temporal coincidence between reduction of repair DNA capacity, increase of cellular damages and mutations and aging with high incidence of malignant tumors in human beings.

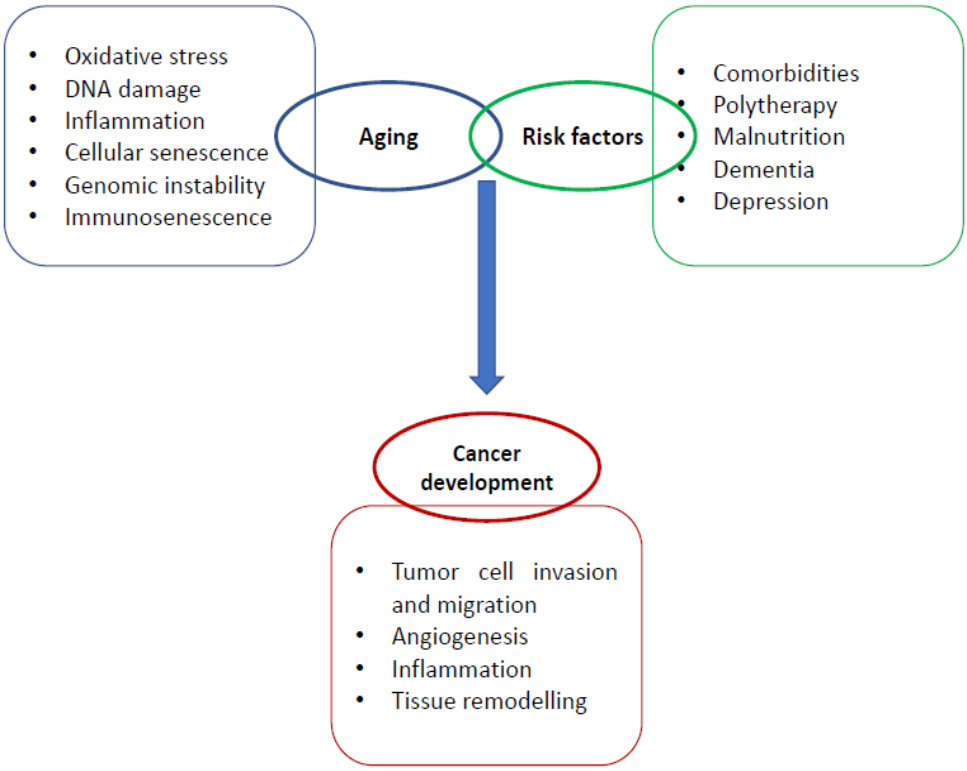

Figure 2. Relationships between aging and cancer.

Another age-related factor that can stimulate tumor growth is represented by immunosenescence. In fact with aging the immune system progressively becomes less effective and, consequently, less able to counteract tumor development (Muller L. et al., 2019).

1. Chemotherapy and Chemoresistance

1.1. Chemotherapy

Chemotherapy consists in the administration of cytotoxic drugs in order to eradicate or reduce the tumor. These compounds, by acting preferentially on rapid-proliferating cells, efficaciously induce cancer cell death, therefore decreasing the tumor-related symptoms and prolonging patient's life expectancy.

The initial success of early chemotherapeutic drugs (such as Nitrogen Mustard and Aminopterin) in the treatment of patients with lymphoma was quickly overcome (Farber S., 1948) by the toxic effects induced by nitrogen mustards on the lymphatic system observed during the Second World War. However, although a rapid tumour relapse was found after an initial antitumor effect, this experience gave rise to the birth of anticancer chemotherapy (Gilman A., 1963).

1.1.1. Classification of chemotherapeutics

Chemotherapeutic drugs are traditionally classified by considering their mechanism of action (Table 1; Williams D.A., 2005):

Drug	Mechanism of action
Cyclophosphamide	DNA alkylation
Methotrexate, 6-thioguanine, 5-fluorouracil	Antimetabolite
Actinomycin D, Doxorubicin	Antibiotic
Vinka alkaloids	Antimitotic
Etoposide, Teniposide	Topoisomerase inhibitor

Table 1. Classification of chemotherapeutic drugs.

Several are the therapeutic plannings through which chemotherapy is administered:

- *induction therapy:* the aim is to reduce the tumor mass as much as possible and to achieve positive clinical effects;
- *adjuvant therapy:* chemotherapy is administered after tumor resection or radioterapy, with the aim to eradicate any residual cancer cell that could give rise to metastatic process;
- *pre-operative therapy:* chemotherapy is given prior to surgical resection in order to reduce the mass of the tumor that cannot be surgically operated;
- *neo-adjuvant therapy*: it is given before surgery or before radio- or chemotherapy with the aim to reduce cancer mass in order to reach a better therapeutic response;

1.1.2. Topoisomerases and their inhibitors

DNA Topoisomerases, highly conserved nuclear enzymes essential for the survival of all eukaryotic organisms, are able to induce transient DNA strand breaks and to catalyze DNA relaxation/supercoiling, catenation/decatenation and knotting/unknotting (Bates A.D. et al., 1997; Wang J.C., 2002). These enzymes, which are involved in replication, transcription, chromosome separation and segregation (Nitiss J.L., 2009), are grouped in two classes: Topoisomerase I able to make DNA single-strand breaks and Topoisomerase II responsible for DNA double-strand breaks (Kellner U. et al., 2002).

Two homologous isoforms of Topoisomerase II exist: alpha (α) and beta (β). The α isoform is targeted by Etoposide (Gatto B., 2003), a natural compound that

together with teniposide, anthracyclines and mitoxantrone has been approved by FDA as topoisomerase II inhibitor.

1.1.3. Podophyllotoxins and Podophyllotoxin Analogues: Etoposide

The first successful anticancer agent targeting topoisomerase II was Etoposide (Fig. 3, 4), which is obtained by podophyllotoxin, a natural product found in the plant *Podophyllum Peltatum*.

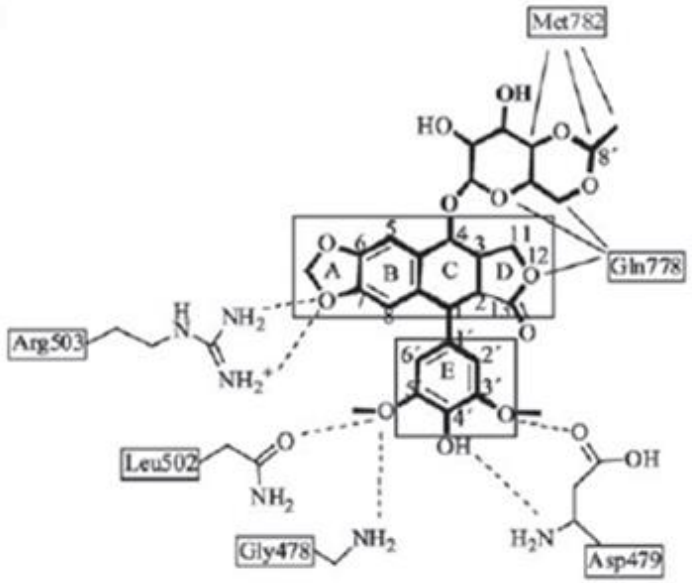

Figure 3. 2D representation of the Etoposide molecule in the active site of the topoisomerase II enzyme. Etoposide consists of a polycyclic core, formed by 4 rings (A-D) linked to benzene, and by a glycosidic group at the C-4 position (Pogorelcnik B. et al., 2013).

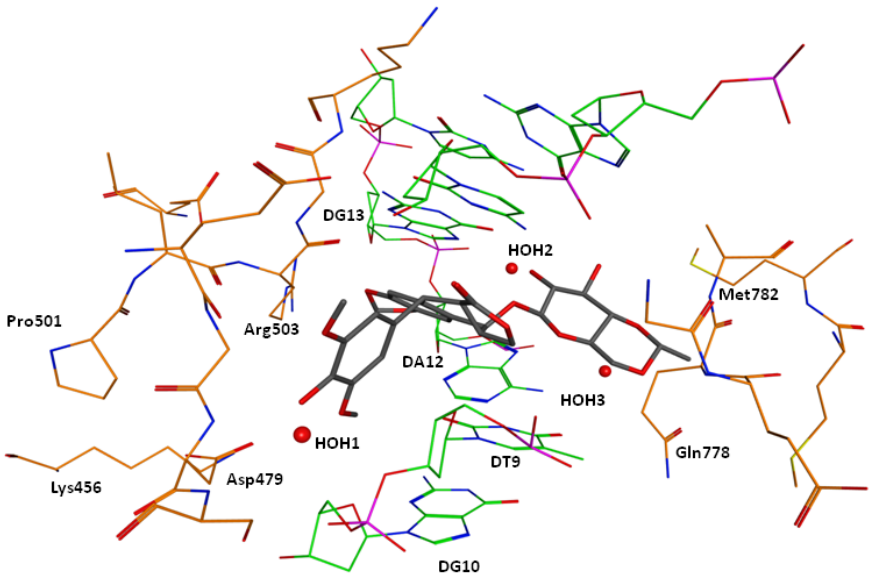

Figure 4. 3D representation of the Etoposide molecule in the active site of the topoisomerase II enzyme. The 3D image, obtained through the Molecular Operating Environment (MOE) modeling program, shows the interactions between Etoposide and Topoisomerase II. Etoposide interacts with arginine 503, aspartate 479, methionine 782 and glutamine 778 present into the active site of the enzyme with three molecules of water and with nitrogenous bases deoxyadenine 12, deoxyguanine 13, deoxyguanine 10 and deoxytimine 9 of DNA.

Etoposide has been clinically used for more than twenty years and remains one of the most prescribed cancer drugs in the world to treat several kinds of malignancies such as testicular cancer, small cell lung cancer, lymphomas, sarcomas and ovarian cancer.

Etoposide is poorly water-soluble and it is dissolved in a solution composed of polysorbate 80, polyethylene glycol and alcohol and than diluted to a concentration less than 0.4 mg/ml to avoid precipitation. The presence of these additives may be the responsible for the hypersensitivity reactions which occasionally appear during Etoposide infusion (Veal G.J. et al., 2006).

Although the most serious adverse event associated with Etoposide exposure is the development of acute myelogenous leukemia (Smith M.A. et al., 1999), it

also induces several secondary toxic effects such as bone marrow suppression, nausea, vomiting and alopecia, liver toxicity, fever and chills.

1.2. Chemoresistance

Chemoresistance is the ability of cancer cells to survive under therapeutic regimen and therefore it is the main cause for cancer recurrence and unfavorable clinical outcome. Moreover chemoresistance, by inducing patient's refractoriness versus several drugs, can lead to the acquisition of multidrug resistance (Ford J. et al., 1990).

Chemoresistance is due to many reasons including the tumor type, the inter-individual patient's variability (Larsson R. et al., 1993), the tumor microenvironment, the drug availability in terms of drug efflux and inactivation, the cell death inhibition, alterations of DNA damage repair, the presence of cancer stem cells (CSCs) and the acquisition of epithelial mesenchymal transition state (Fig. 5).

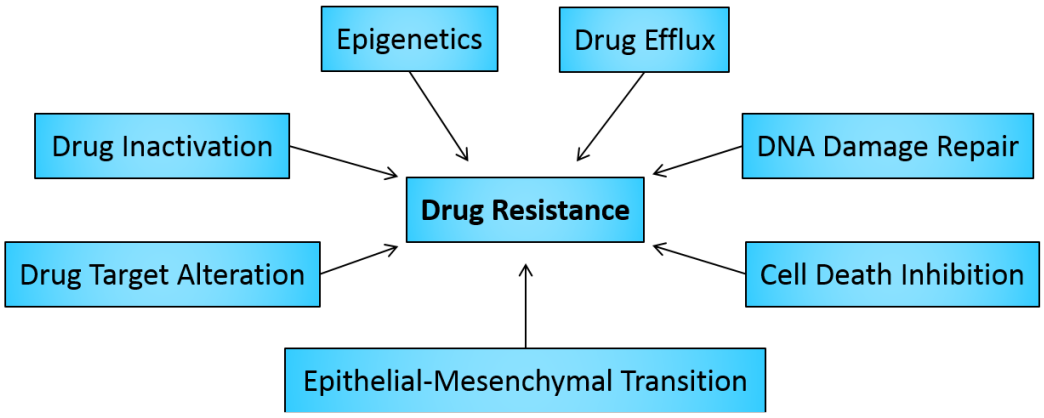

Figure 5. Mechanisms that concur to promote drug resistance in human cancer cells. These mechanisms can act independently or in combination by modulating several signal transduction pathways involved in cell survival and death (Housman G. et al., 2014).

1.2.1. Mechanisms of chemoresistance

1.2.1.1. Tumor microenvironment

The tumor microenvironment (TME) plays a crucial role in the progression of more advanced and therapy-refractory cancers (Mroue R., 2013; Chen F. et al., 2015). The relationship between micronvironment and cancer was identified in the second half of 19th century by Rudolf Virchow who firstly proposed the link between chronic inflammation and tumor growth (Balkwill F., 2001).

The TME is composed by cellular components such as cancer-associated fibroblasts (CAFs), mesenchymal stromal cells (MSCs), adipocytes, endothelial cells, immune and inflammatory cells (Bharti R. et al., 2016) and non-cellular components such as extracellular matrix (ECM), matrix remodeling enzymes, cytokines, growth factors and inflammatory enzymes (Tan S. et al., 2020; Patel H. et al., 2018). In contrast to healthy microenvironment that contains vascular networks able to guarantee an adequate supply of oxygen and growth factors and to remove metabolic waste products (Hanahan D., 1996), the TME is characterized by an aberrant vasculature and produces a condition of hypoxia, matrix rigidity and an altered composition of paracrine factors (Fig. 6).

It has been shown that, as a consequence of a big consumption of oxygen by rapidly proliferating cells and an inadequate vasculature, many cancers are characterized by a hypoxic microenvironment that can antagonize the effect of cancer treatments. Hypoxia results in the activation of hypoxia-inducible transcription factors (HIFs) and many downstream target genes (Doktorova H. et al., 2015).

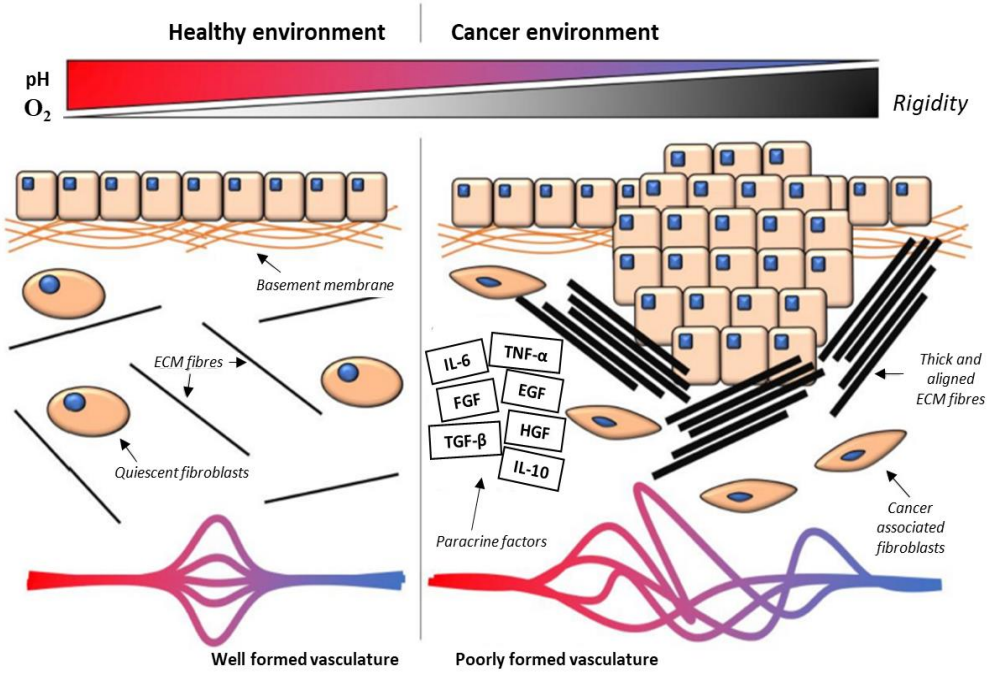

Figure 6. Differences between healthy and cancer microenvironment (Yeldag G. et al., 2018). In the healthy environment, the basement membrane separates epithelial cells from the stroma which is characterized by quiescent fibroblasts and low abundance of ECM fibers which contribute to reduce stromal rigidity. The vasculature is highly organized, and there is a high level of oxygen and a neutral pH. In the cancer environment, the invasive cell growth leads to basement membrane disruption and to the consequent contact between cancer cells and highly rigid stroma. The vasculature although excessive is poorly organized, and oxygen and pH are reduced. TNF-α = tumor necrosis factor alpha, IL-6 = interleukin 6, IL-10 = interleukin 10, EGF = epidermal growth factor, FGF = fibroblast growth factor, HGF = hepatic growth factor, TGF-β = transforming growth factor beta.

With regard to paracrine factors, epidermal growth factor (EGF), fibroblast growth factors (FGF) and platelet derived growth factor (PDGF) are highly present in the TME (Hanahan D. et al., 2012).

Moreover, pro-angiogenetic factors (e.g. vascular endothelial growth factor, VEGF) are very abundant in the TME and stimulate a production of a disorganized vasculature, with immature and hyperpermeable vessels (Jung Y. D. et al., 2000; Siemann D.W., 2011).

The extracellular matrix (ECM) is not only a simple intercellular filling, but rather a physiologically active component of the tissue, responsible for cell–cell communication, adhesion and proliferation (Frantz C. et al., 2010; Brown N.H., 2011). Although the ECM composition is specific for each tissue, the common components are represented by water, minerals, proteoglycans and fibrous proteins such as collagen, laminin and fibronectin secreted by resident cells (Frantz C. et al., 2010; Bonnans V., 2014). The ECM is a highly dynamic structure and it is particularly involved in physiological processes such as wound healing, angiogenesis and bone remodelling (Gattazzo F. et al., 2014; Rohani M.G., 2015).

During carcinogenesis, the molecular talk between ECM and cancer cells sustains ECM architectural changes by favoring cancer cell growth and spread (Malik R. et al., 2015).

1.2.1.2 Drug Availability and Drug Efflux

Drug availability is the ability of the drug to reach its cellular target and it can be altered by several mechanisms. In fact, after their entry into the cells, drugs can be inactivated by cytochrome P450 system (CYP), glutathione-S-transferase (GST) or uridine diphospho-glucuronyltransferase (UGT) (Michael M. et al., 2005).

Besides, cancer cells may colonize and proliferate in ‘sanctuary sites’ (such as bone marrow) or in anatomical spaces in which drugs are unable to reach adequate therapeutic concentrations. In this regard, the prototype example is represented by the central nervous system (CNS) due to the presence of the blood–brain barrier. As a consequence of several drugs unable to bypass the blood–brain barrier, melanoma, lung, HER2-positive breast and kidney cancers show high CNS tropism (Valiente M. et. al., 2018).

Drug efflux is mediated by the ATP binding-cassette (ABC) superfamily that is the largest family of membrane transporters able to sustain the endogenous and exogenous substrates trafficking across cell membranes (Morales M., 2017; Hamed A.R. et al., 2019). Due to their role, ABC transporters can play a crucial role in the onset of chemoresistance (Wang X. et al., 2019) (Fig. 7). With this regard, ABC proteins have been found overexpressed in several multi-drug-resistant cancers (Table 2) (Perez-De Marcos J.C. et al., 2021).

Table 2: ABC overexpression in cancer

ABC1	Glioma, Lung cancer
ABC2	Liver cancer, Leukemia
MRP4	Neuroblastoma
ABC8	Breast, Renal, Lung cancer

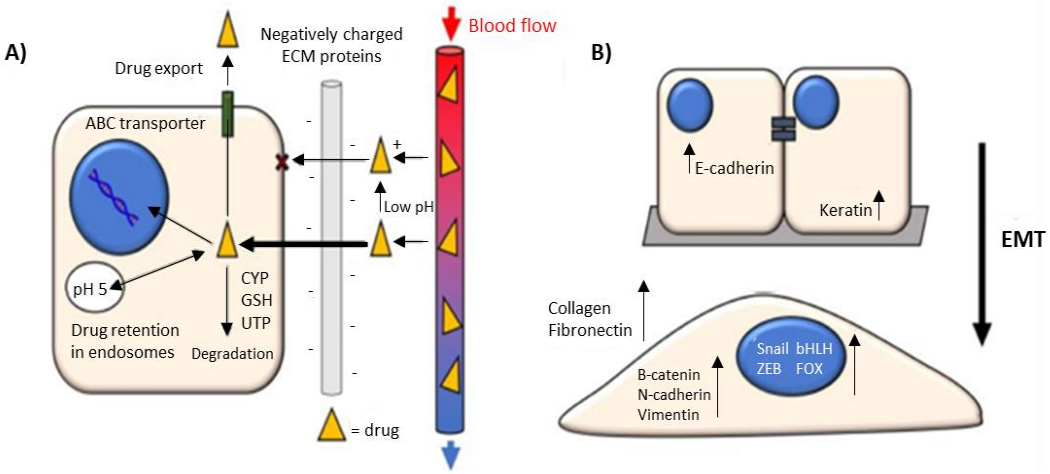

Figure 7. Mechanisms of chemoresistance (Yeldag G. et al., 2018).
A) Drug availability. Drugs (yellow triangles) move from blood vessels to cells. Low pH levels can promote charged drugs that interact with negatively-charged extracellular matrix (ECM) components (grey), slowing their transit. Alternatively, drugs can be transported out of the cell by ABC transporters, and degraded by the cytochrome P450 system (CYP), glutathione-S-transferase (GSH) superfamily or uridine diphospho-glucuronosyltransferase (UGT) superfamily. Drugs also enter endosomes, and charged drugs are retained more within these acidic vesicles. (B) The epithelial–mesenchymal transition (EMT) process involves the loss of cell–cell adhesion from the epithelial phenotype (above) to the mesenchymal phenotype (below). E-cadherin and keratin characterize epithelial phenotype, while β-catenin, N-cadherin, and vimentin, and the transcription factor families Snail, ZEB, bHLH, and FOX, are more abundant in the mesenchymal phenotype. Collagen and fibronectin secretion is also increased in the mesenchymal phenotype.

1.2.1.3 Cancer cell plasticity and dormancy

Plasticity is the ability of cells to acquire different phenotypes and it is important for tissue regeneration and to mediate response to environmental stimuli.

The contribution that plasticity gives to tumor growth has been described by two models: the first one suggests that different tumor types derive from different cancer cells; the second one hypothesizes that the same original cancer cell may promote the development of different malignant cancer phenotypes through a plasticity process due to genetic alterations and dynamic epigenetic changes

(Yuan S. et al., 2019). Moreover, intrinsic cellular plasticity has also been involved in cancer dormancy, the time period during which patients do not show any symptoms before cancer relapse. Two models of dormancy have been elaborated: the first one, named ‘tumor mass dormancy’, which is characterized by an interruption of tumor growth due to the balance between proliferation and cell death and that could be associated with angiogenic and immunologic dormancy (Folkman J., 2002; Uhr J.W. et al., 2011). The second model, known as “cellular dormancy or solitary cell dormancy”, is referred to the ability that a single cancer cell has to temporarily arrest its cell cycle (Massague J., 2004; Aguirre-Ghiso J.A., 2007).

Plasticity and dormancy are two fundamental biological states that are present in CSCs and are responsible for their chemoresistant phenotype and metastatic potential through epigenetic alterations, metabolic reprogramming and complex interactions with the immune system.

Noteworthy, dormancy has been frequently found in chemoresistant neuroblastoma, a highly aggressive pediatric tumor. Indeed, the dormant phenotype can remain silent for decades as reported in a clinical case of a patient who had a late relapse of metastatic NB 52 years after diagnosis (Kushner B.H. et al., 1986; Mir R. et al., 1987).

1.2.1.4 Epithelial mesenchymal transition

Epithelial mesenchymal transition **(**EMT) is a process where cells switch from an epithelial phenotype, characterized by cell polarity and cell–cell adhesion, to a mesenchymal phenotype, by facilitating cell migration, invasiveness and by increasing resistance to apoptosis. Mesenchymal cancer cells are elongated and highly contractile, and this particular phenotype facilitates their migration through the matrix towards blood vessels or the lymphatic system during metastasis (Parri M., 2010).

EMT process starts with the loss of cell–cell contacts such as the tight junctions, adherens junctions, desmosomes and gap junctions (Lamouille S. et al., 2014). The mesenchymal phenotype is often highly associated with cancer stem cells and chemoresistance.

2. Cancer Stem Cells

Cancer is characterized by an uncontrolled proliferation of morphologically and functionally different malignant cells. The heterogeneity within tumors can be explained by two different models (Reya T. et al., 2001) (Fig. 8):

- 'The Traditional Model' is due to a sequential accumulation of mutations that lead cells to a more primitive phenotype by making them more easily adaptable to microenvironment conditions. In this clonal evolution model, each cancer cell has a similar potential to develop a tumor.
- 'The Cancer stem cell Hypothesis' supposes that a small group of stem-like cells (CSCs) is responsible for the development of the neoplasm. Therefore, these cancer cells with stemness properties are responsible for the generation of a progeny of highly proliferative cells making the bulk of the tumor (Aguilar-Gallardo C. et al., 2013; Pattabiraman D.R. et al., 2014).

However, the two models are not mutually exclusive and can be interpreted as integrated processes since CSCs can undergo a clonal evolution leading to a second more dominant population of CSCs. In fact CSCs, named tumor-initiating cells as well, are a subpopulation of neoplastic cells characterized by an asymmetrical division: a CSC divides into two daughter cells of which one remains a CSC (self-renewal) while the other one differentiates to a neoplastic cell (Pattabiraman DR. et al., 2014).

CSCs share several properties with normal stem cells including the expression of surface stemness markers such as CD44, CD133 or aldehyde dehydrogenase (ALDH) (Pattabiraman D.R. et al., 2014).

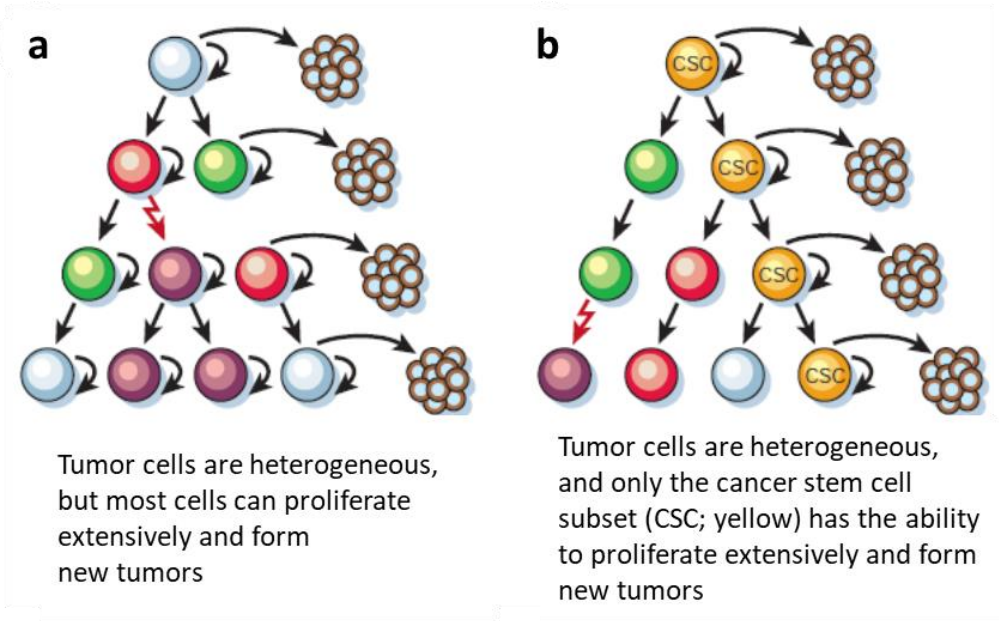

Figure 8. **Two models to explain the heterogeneity of cancer cells.** a) traditional model and b) cancer stem cell model (Reya T. et al., 2001).

CSCs are resistant to conventional anticancer therapies and, for this reason, they are responsible for tumor recurrence and metastasis formation. The therapy refractoriness of CSCs may be due to their low proliferative rate (Anjomshoaa A. et al., 2009; Moore N. et al., 2011). However, it has been observed that CSCs, generally considered quiescent or slow-cycling cells, can re-enter into the cell cycle after radiation exposure during radiotherapy (Lagadec C. et al., 2009).

The traditional cancer therapies acting on cancer cells but not on CSCs, after an initial remission, can lead to cancer relapse (Fig 9). Therefore, a multimodal targeted approach as a combination of CSC-targeted therapies and traditional therapies is needed in order to counteract tumor growth and the onset of therapy resistance (Lu Han et al., 2013; Peiris-Pages M. et al., 2016; De Francesco E.M. et al., 2018).

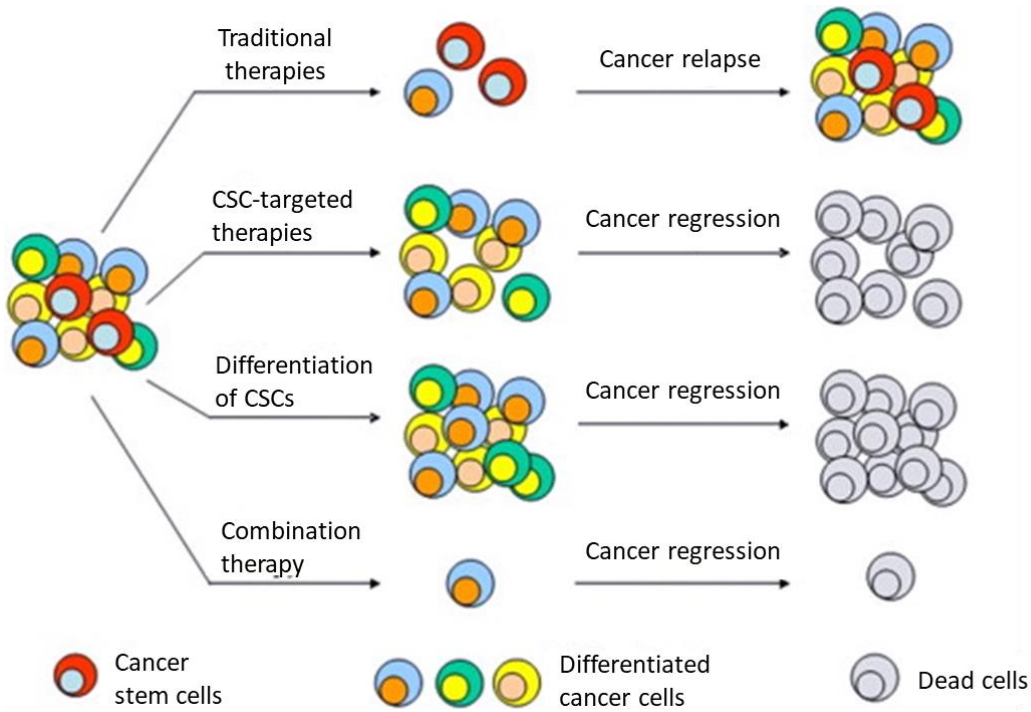

Figure 9. Efficacy of the combined therapy in comparison with traditional cancer therapy and CSC-targeted therapy (Lu Han et al., 2013). The combination of CSC-targeted therapy and traditional therapy may have the benefit of the increased efficacy since it depletes CSCs and kills differentiated cancer cells.

2.1. Cancer stem cell metabolism

Under normoxic conditions cells produce energy *via* oxidative phosphorylation (OXPHOS), which is more efficient than glycolysis since it generates 36 molecules of ATP/molecule of glucose while glycolysis produces only 2 molecules of ATP/molecule of glucose. Nevertheless, cancer cells choose to generate ATP mainly *via* glycolysis even in the presence of oxygen: the phenomenon is known as Warburg effect or aerobic glycolysis (Guppy M. et al., 1993).

With regard to CSCs, it has been demonstrated that they have higher glucose uptake and an increase in glycolytic enzymes, lactate production and ATP content

in comparison to cancer cells. However, although conflicting hypotheses have been reported (De Luca A. et al., 2015; Farnie G. et al., 2015), the prevalence of the glycolytic phenotype seems to be correlated to a reduction in mitochondrial oxidative metabolism (Fig. 10) (Peiris-Pagès M. et al., 2016; Liao J. et al., 2014; Zhou Y. et al., 2011). One probable reason for the discrepancies found in CSC metabolism may be due to their metabolic adaptability to microenvironmental changes. In fact, while in most *in-vitro* studies carried out under non-physiological glucose and oxygen concentrations the glycolytic phenotype is prevalent, in patient-derived CSC OXPHOS is the preferred metabolic pathway (Vlashi E. et al., 2011).

Moreover, it has been shown that different subpopulations of CSCs exhibit different metabolic patterns, by suggesting that the choice of a specific metabolic pathway to produce energy may depend on the tumor/metastasis site (Dupuy F. et al., 2015).

Therefore, in order to eradicate CSCs, a promising effective strategy could be to simultaneously inhibit glycolysis and mitochondrial respiration rather than to inhibit only one of two metabolic pathways (Cheong J.H. et al., 2011).

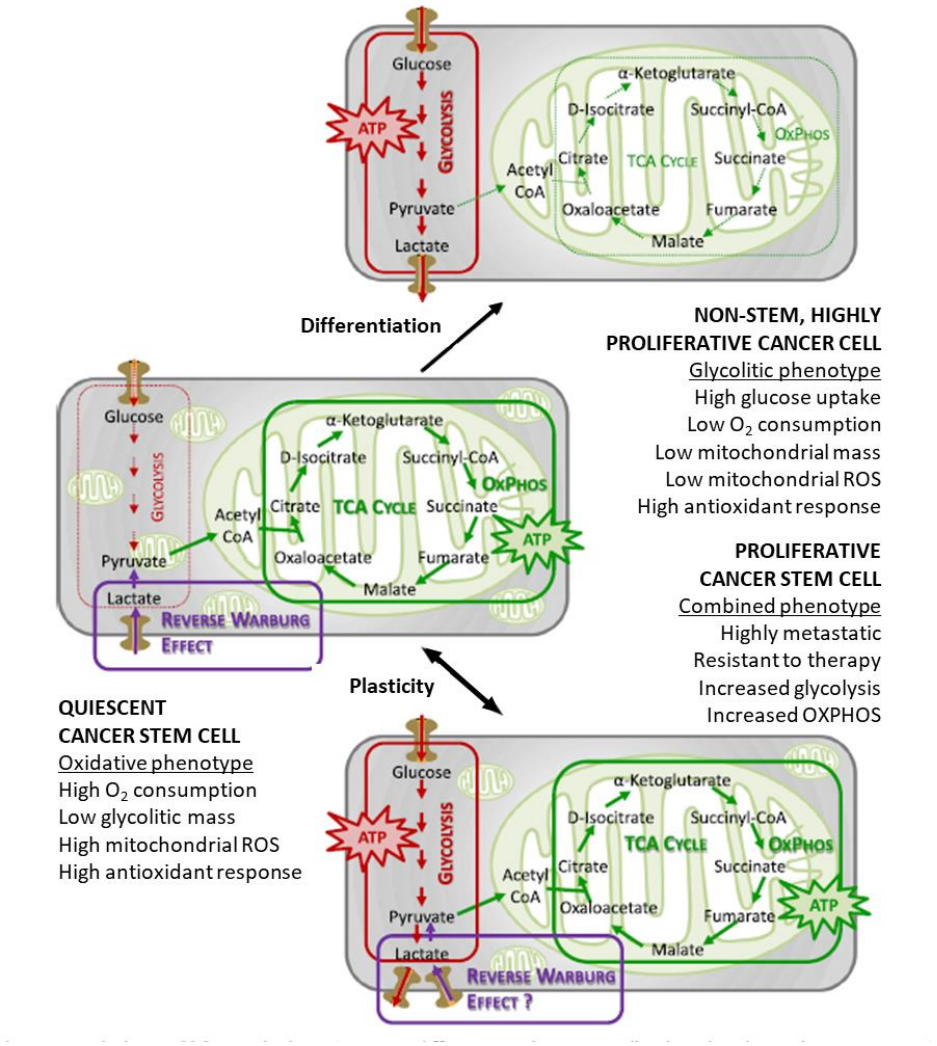

Figure 10. Energetic pathways in CSCs (Peiris-Pagès M. et al., 2016). In cancer cells, the glycolytic phenotype may predominate over OXPHOS. CSCs may depend on an oxidative metabolism for ATP production. CSCs also appear to be metabolically plastic: when OXPHOS is blocked they can develop resistance by acquiring a glycolytic/oxidative phenotype.

2.2 Cancer stem cells and Epithelial–mesenchymal transition (EMT)

The acquisition of stem cell traits by both healthy and neoplastic cells is associated with the EMT process (Mani S.A. et al., 2008; Morel E.P. et al., 2008; Sheridan C. et al., 2006).

Recent studies report that CSCs exist in distint mesenchymal like (epithelial-mesenchymal transition; EMT) and epithelial-like (mesenchymal-epithelial; MET) states that may be interconvertible (Liu S. et al., 2015). Notably, important differences between the two phenotypes have been described in breast cancer: MET CSCs are characterized by an enhanced proliferative capacity whereas EMT CSCs are characterized by a slow-cycling and by a quiescent state. EMT CSCs seem to prefer glycolysis and have a marked reduction in oxygen consumption, decreased mitochondrial mass and membrane potential, lower ROS production and higher antioxidant defense in comparison with MET CSCs (Gammon L. et al., 2013).

EMT programs are regulated by a set of transcription factors that facilitate the local invasion and subsequent propagation of cancer cells to distant sites (Scheel C. et al., 2012). In fact, cells that undergo EMT change the expression of adhesion-proteins gene by down-regulating those ones favoring the epithelial phenotype such as *E-cadherin*, *Claudin* and up-regulating those ones that stimulate mesenchimal state such as *Snail* (Cano A. et al., 2000), *Slug* (Bolos V. et al., 2003) and *Zeb1* (Eger A., et al., 2005).

Cadherins are a family of proteins that mediate cell-cell adhesion and play crucial roles in tissue development. In detail, *E-Cadherin* is a transmembrane protein (Chung J.H. et al., 2010) highly expressed in focal adhesions where it plays an important role in the maintenance of morphological and structural integrity of

epithelial cells. A low level or the absence of *E-cadherin* reduces cancer cell adhesion by facilitating the metastatic process. In addition, it has been reported that the loss of *E-cadherin* in cancer cells has been associated with an up-regulation of *N-cadherin* confirming that this "cadherin switch" is one of the hallmarks of EMT process (Aigner K. et al., 2007**).** As *N-cadherin*, the up-regulation of *Vimentin*, an intermediate filament of mesenchimal origin, is associated to the EMT process.

Claudin and *Occludin*, that guarantee cellular permeability and polarity by joining the cell junctions to the cytoscheletron, are downregulated during EMT (Oliveira S.S., 2007). Another EMT facilitating protein is *β-catenin*, a key effector of Wnt-dependent signalling pathway that, by activating *Slug*, binds to E-cadherin promoter repressing its gene transcription and contributing to reduce cell adhesion. Down-regulation of *E-cadherin* is also induced by *ZEB1* which is a recognized transcription factor able to promote tumor progression and metastasis formation (Peijing Z. et al., 2015).

In this regard, Brabletz T. demonstrated that ZEB1 is a crucial EMT inducer in human carcinoma (Brabletz T. et al., 2010). In fact, its expression is associated with a selective loss of basement membrane in invasive epithelial cancers (Spaderna S. et al., 2008; Thiery J.P. et al., 2009; Brabletz S., 2012). Therefore, ZEB1 has been found to be a strong predictor of poor patient survival and metastasis formation. Based on his studies, Brabletz proposed the "migrating cancer stem cell" concept in which EMT phenotype of cancer cells at the invasive front might include migrating cancer stem cells (Brabletz T. et al., 2005)

Moreover, ZEB1 has a dramatic impact during all phases of carcinogenesis (Fig. 10). In fact, aberrant expression of ZEB1 has been observed in several human cancers, such as osteosarcoma (Shen A. et al., 2012), uterine (Spoelstra N.S. et al.,

2006) and breast cancer (Eger A. et al., 2005). Since in some cancer cell lines (colon, lung, and breast cancer) the over-expression of ZEB1 enhances invasive and migratory capacities *in vitro* and metastasis formation *in vivo*, there is increasing evidence that functions of ZEB are not limited to EMT modulation. Indeed, ZEB might participate in a central switch that controls critical cellular functions and states, including differentiation, proliferation, response to DNA damage and cell survival with a dramatic influence on tumor growth (Fig. 11) (Puisieux A. et al., 2014).

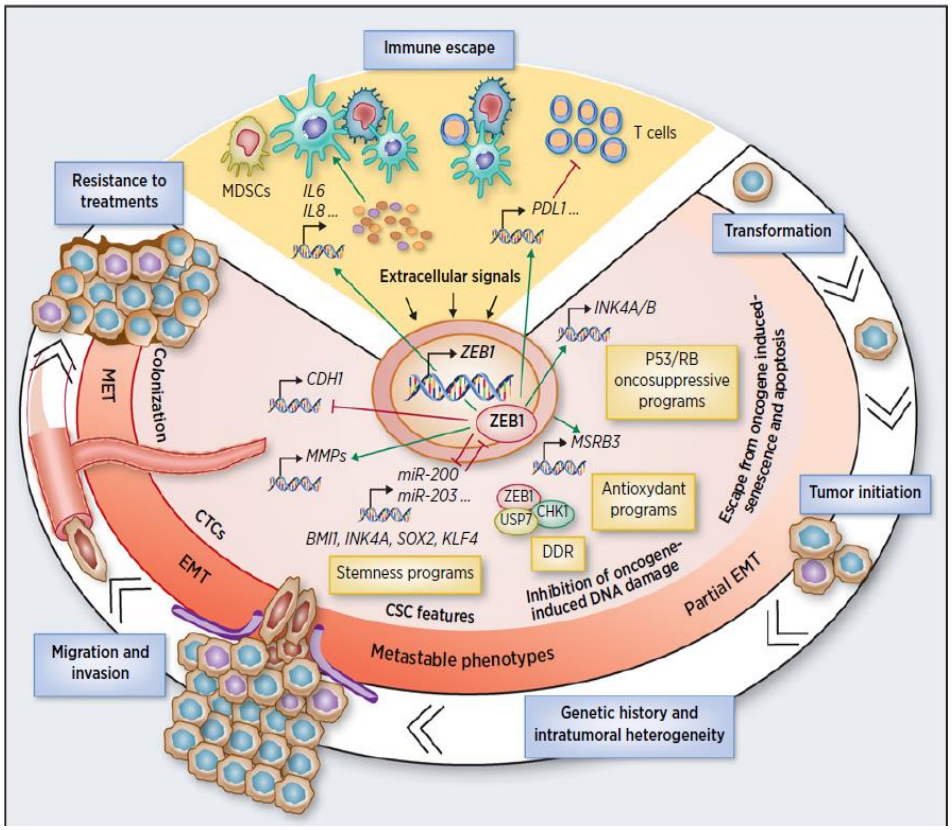

Figure 11. Oncogenic functions of the transcription factor ZEB1 which is a central determinant of cell fate. It regulates the activity of transcription factors involved in the control of cell differentiation, proliferation, survival and motility. ZEB1 also promotes cancer immune escape and contributes to drug resistance (Caramel J. et al., 2018).

3. Cellular Antioxidant defense mechanisms

Aerobic organisms produce ATP mainly *via* oxidative phosphorylation (OXPHOS). Proteins of the electron transport chain, located in the inner mitochondrial membrane, through a series of redox reactions, transport electrons from nicotinamide adenine dinucleotide hydrogen (NADH) to oxygen (O_2), the terminal electron acceptor which is then reduced to H_2O. NADH is one of the main metabolites obtained from the tricarboxylic acid (TCA) cycle that takes place within the mitochondrial lumen and that is driven by acetyl-CoA derived from glycolysis and oxidation of fatty acids (Papa S. et al., 2012). During the electron transport, a small percentage of electrons escapes and reacts with the oxygen molecules giving rise to highly reactive superoxide molecules ($O_2^{-\cdot}$). For this reason, OXPHOS is the major source of reactive oxygen species (ROS) that are able to cause oxidation of proteins, lipids, sugars and DNA.

In order to counteract these oxidant species and consequently to survive, cells have developed a complex antioxidant defense system.

The most representative antioxidants include either enzymatic systems, such as superoxide dismutase, catalase, glutathione peroxidase, glutathione reductase, and non enzymatic molecules such as GSH, vitamins A, C and E (Marengo B. et al., 2016).

Superoxide dismutase

Superoxide dismutases (SODs) catalyze a dismutase reaction that converts superoxide to oxygen and hydrogen peroxide:

$$2O_2^{-\bullet} + 2H^+ \rightarrow O_2 + H_2O_2$$

An excess of superoxide production plays a crucial role in the pathogenesis of many pathological conditions including cancer (Fukai T. et al., 2011; Miao L. et al., 2009).

Catalase

Catalase is an enzyme whose main function is to eliminate hydrogen peroxide by catalyzing its dismutation to oxygen and H_2O through a two-step reaction (Powers S.K. et al., 2008). The final reaction is the following:

$$2H_2O_2 \rightarrow 2H_2O + O_2$$

3.1. Glutathione

Glutathione is a tripeptide, composed of cysteine, glycine and glutamic acid, which is found in millimolar concentrations in most cells (Fig. 12). Glutathione exists as reduced (GSH) and oxidized (GSSG) form and the ratio between them determines the cellular redox state.

GSH is widely distributed in all organisms and has several important functions (Sies H., 1999) such as the ability to inactivate xenobiotics and toxic endogenous compounds by linking them *via* conjugation reactions spontaneously or enzymatically, by means of GSH-transferase (GST) activity (Meister A., 1988). Moreover, GSH plays a crucial role in cellular antioxidant defence and its depletion, by increasing ROS production, can induce DNA damage, lipid peroxidation and protein denaturation (Martin H.L. et al., 2009).

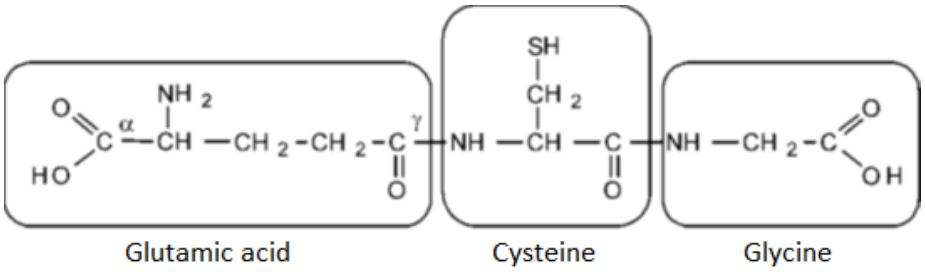

Figure 12. Chemical structure of glutathione.

Moreover, GSH is a fundamental co-factor for several GSH-related antioxidant enzymes such as GPX, GST and GSR.

Glutathione peroxidase

Glutathione peroxidase (GPX) is a family of enzymes that reduce H_2O_2 or hydroperoxides to H_2O or alcohols through the oxidation of two molecules of GSH.

$2GSH + H_2O_2 \rightarrow GSSG + 2H_2O$

$2GSH + ROOH \rightarrow GSSG + ROH + H_2O$

In mammals, GPX family consists of eight distinct selenoproteins and among them GPX6 is found only in humans (Brigelius-Flohe et al., 2013; 1999).

Unlike other GPXs, GPX4 has a higher substrate preference, being able to directly reduce phospholipid hydroperoxides (Ursini et al., 1982). In fact GPX4, by reducing the hydroperoxide group (-OOH) of esterified fatty acids in membrane phospholipids, can prevent lipid peroxidation (Maiorino M. et al., 2018; Cozza G. et al., 2017; Ingold I. et al., 2018). GSH is the co-factor of GPX4 (Mannervik B., 1985) and its depletion, by directly inactivating GPX4, can lead to '*ferroptosis'*, a recently identified form of cell death (Yoo S. et al., 2012; Friedmann A.J.P. et al., 2014; Friedmann A.J.P. et al., 2018).

GPX4 is present as mitochondrial, nuclear and cytosolic isoforms, even if only the cytosolic isoform is required for the prevention of ferroptosis (Ursini and Maiorino, 2020).

Glutathione-S-Transferase

Another enzyme involved in the detoxification of oxidized substrates is Glutathione-S-transferase (GST) which catalyzes the conjugation of GSH with oxidized substrates or xenobiotics that are subsequently eliminated.

Glutathione reductase

Glutathione reductase (GR) is an enzyme able to convert GSSG to GSH by using NADPH and flavine adenine dinucleotide (FAD), a derivative of the riboflavin (Fig. 13).

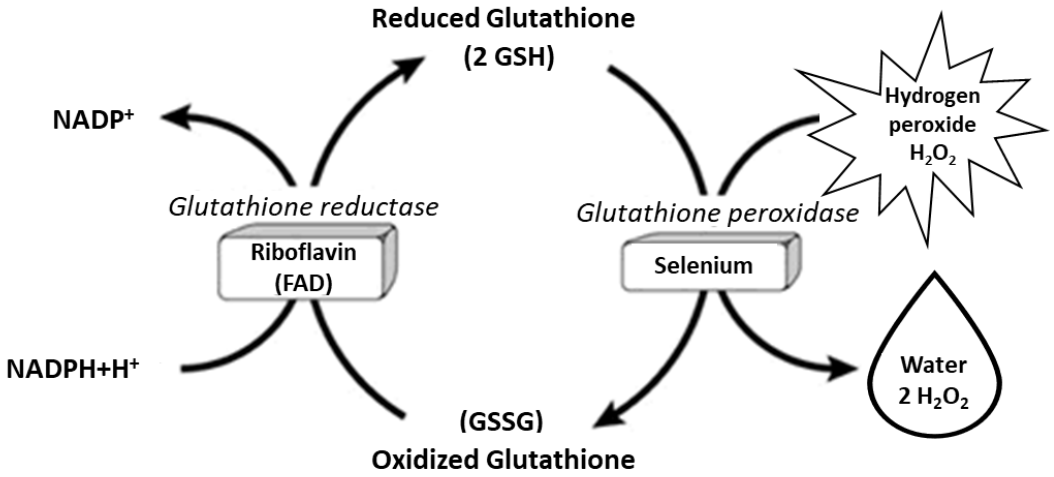

Figure 13. Conversion of GSSG to GSH by Glutathione Reductase (Ilkhani F. et al., 2016).

4. GSH and Cancer Stem Cells: role of xCT system and CD44

xCT, the cystine/glutamate antiporter solute carrier family 7 member 11 (SLC7A11), is an antiport transporter that mediates glutamate efflux and uptake of cystine which is a crucial aminoacid used for GSH biosynthesis (Lo M., et al., 2008). Recent studies have demonstrated that xCT can play an important role in tumor growth, progression, metastasis formation and in the acquisition of multidrug resistance (Fig. 13; Liu J. et al., 2020).

The xc (-) system is composed of two different subunit chains: a light chain (xCT or SLC7A11) and a heavy chain (CD98hc or SLC3A2). The transcription of xCT is induced by oxidative stress or cystine depletion and is mediated by the binding of Nfr2 transcription factor to xCT promoter (Sasaki H. et al., 2002). xCT protein has been found to be stabilized at the plasma membrane by CD44, which is a stem cell marker also expressed on the surface of CSCs derived by breast, colon, pancreatic and prostate cancers (Yan Y. et al., 2015).

CD44 is a transmembrane protein which plays an important role in mediating cell adhesion since it is able to interact with hyaluronic acid, one of the main components of the extracellular matrix. CD44 exists in several isoforms which are generated by mRNA alternative splicing (Ponta H. et al., 2003). In detail, the variant CD44v9 is able to stabilize xCT at the plasma membrane and, by increasing cystine uptake, facilitates GSH biosynthesis and consequently blocks ROS-modulated signaling pathways and prevents ferroptosis (Fig. 14) (Masanori H. et al., 2016).

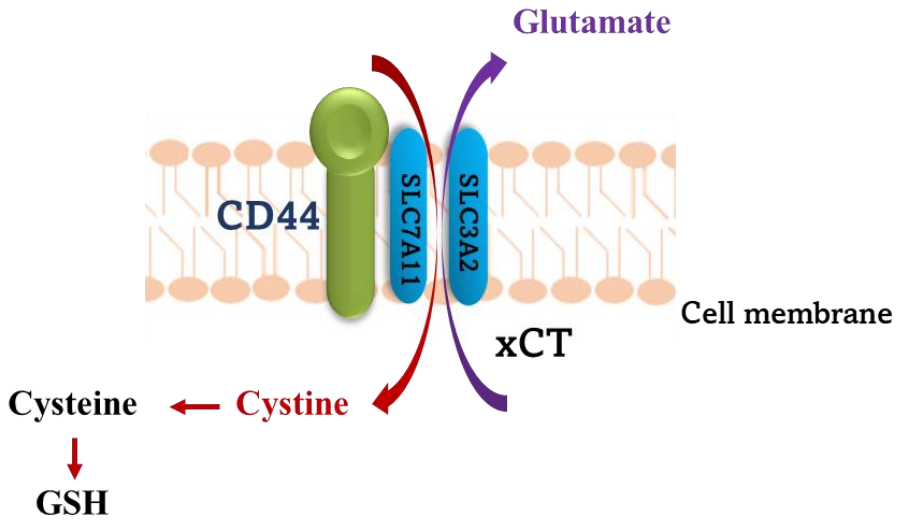

Figure 14. xCT is stabilized in the membrane by CD44v9 and favors cellular uptake of cystine which is crucial for GSH biosynthesis (Ishimoto T. et al., 2011).

CD44 is involved in a wide variety of physiological and pathological processes. The cleavage of CD44 ectodomain is mediated by membrane-associated matrix metalloproteinases (MMPs) and is induced by several stimuli, including extracellular Ca^{2+} influx and the activation of protein kinase C-α (PKC-α) (Kawano Y. et al., 2000). In this context, it has been reported that PKC-α is responsible for the activation of a metalloproteinase 9 which cuts the extracellular domain of CD44, thus activating a γ-secretase responsible for the cutting of CD44 intracellular domain. Then, CD44 can translocate to the nucleus where it stimulates the expression of CD44 gene (Nagano O. et al., 2004), and in particular of CD44v9, which stabilizes xCT in membrane. Therefore, by inhibiting PKC-α, the activation of xCT would be hindered with a significant decrease in GSH content.

Protein kinase C-α (PKC-α)

Protein kinase C-α (PKC-α) belongs to conventional or classic PKC isoforms (Fig. 15) which are serine/threonine protein kinases activated by calcium and phospholipids. PKC-α is composed of 672 amino acids and it is ubiquitously expressed in all tissues (Dempsey et al., 2000). PKC-α is involved in many cellular functions such as proliferation, differentiation, apoptosis, motility and adhesion (Lo L. et al., 2001).

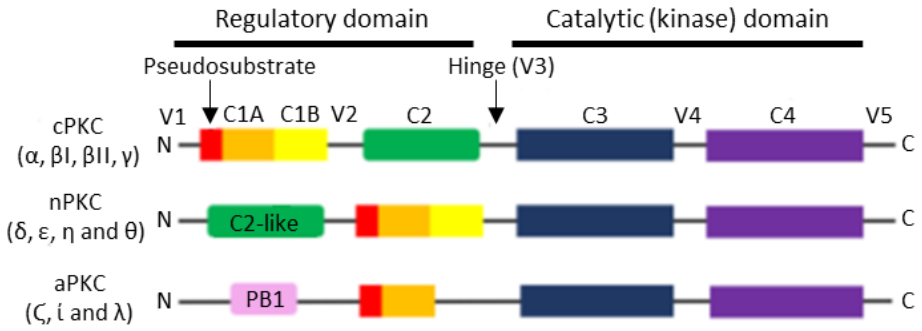

Figure 15. Structure of PKC isoforms. All PKCs consist of a regulatory domain, a catalytic (kinase) domain, and variable regions (V1–V5). The regulatory domain of all PKCs includes a C1 domain and classic PKCs have a C2 domain that binds to calcium. The C3 and the C4 domain of all PKCs bind to ATP and substrate, respectively (Kawano T. et al., 2021).

PKC-α overexpression is implicated in determining aggressive and metastatic malignant phenotypes in breast cancer (Sun X. et al., 1999). Furthermore, PKC-α may also be involved in drug resistance through phosphorylation and activation of membrane efflux pumps, including P-glycoprotein (Ways D.K. et al., 1995).

The involvement of PKCs in cancer supports the idea that PKCs can be direct potential targets for anticancer therapy; in fact, many PKC modulators are used in clinical trials alone or in combination with other compounds. PKC inhibitors include inhibitors of the ATP-binding domain, peptides that inhibit kinase domains and anti-sense oligonucleotides (Kawano T. et al., 2021).

4.1 Sulfasalazine: an xCT inhibitor

Sulfasalazine (SSZ) is a sulfonamide antimicrobial agent obtained by chemical synthesis and not from microorganisms like standard antibiotics. SSZ is a prodrug since it is intrinsically active due to the absence of a para-amino aromatic substituted group; intestinal bacteria convert the prodrug into sulfapyridine and 5-aminosalicylic acid (Fig. 16) which has anti-inflammatory properties (Wahl C., 1998).

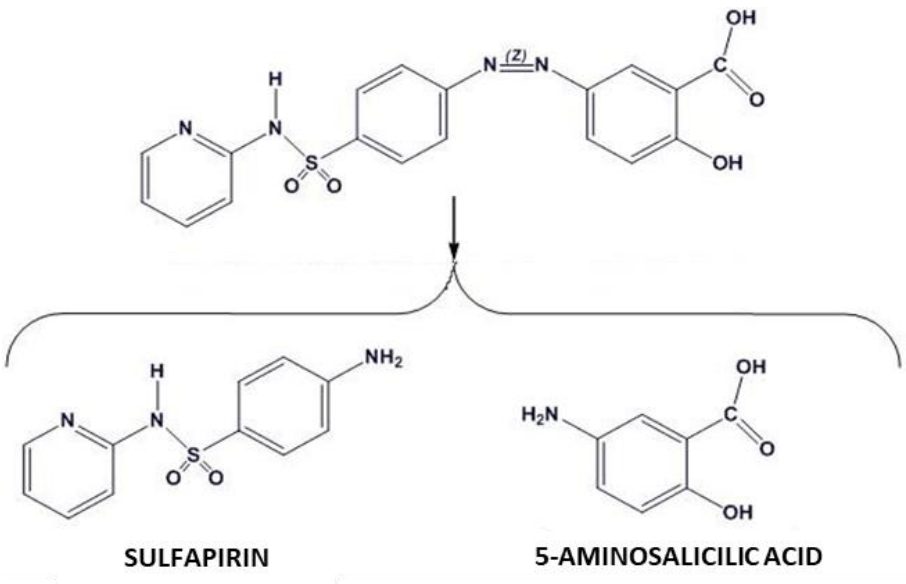

Figure 16. Activation of SSZ to 5-aminosalicylic acid.

Furthermore, SSZ has been recognized as xCT inhibitor which, by limiting cystine uptake, reduces GSH levels and limits tumor growth (Babu KR et al., 2016).

In fact, SSZ has been observed to act as a carboplatin sensitizer in the treatment of brain malignancies. In gliomas xCT is highly expressed and SSZ is effective in inhibiting tumor growth and associated complications (Sontheimer H. et al.,

2012). Recently, it has been observed in colorectal cancer that SSZ associated with cisplatin has a synergistic cytotoxic effect (Ma M.Z. et al., 2015).

Also, in lung cancer xCT is highly expressed and its inhibition with SSZ reduces cell proliferation and invasive capacity both *in vitro* and *in vivo* (Ji X. et al., 2018). Nevertheless, since SSZ has a short half-life and it is transformed into 5-aminosalicylic acid, it is necessary to develop more specific and potent xCT inhibitors with a greater bioavailability (Sontheimer H. et al., 2012).

xCT inhibition induced by SSZ or erastin leads to intracellular GSH depletion and consequently becomes a potent inducer of ferroptosis in cancer cells (Dixon S.J. et al., 2012).

In addition, it has been reported that SSZ, by disrupting the circadian rhythm of transferrin receptor 1 (TFR1) gene expression, could affect iron metabolism (Yoshida G.J., 2018; Okazaki F. et al., 2017) and, consequently, induce ferroptosis (Yamaguchi Y. et al., 2018).

5. Ferroptosis

The term *Ferroptosis* was first coined in 2012 and described as a type of regulated cell death induced by cystine deprivation (Dixon S.J. et al., 2014) that is responsible for intracellular GSH depletion. Moreover, the requirement of GSH to protect cells from ferroptosis was later related to the activity of glutathione peroxidase 4 (GPX4), a selenoprotein required for the efficient reduction of peroxidized phospholipids (Ursini F. et al., 1982; Friedmann A.J.P. et al., 2014; Yang W.S. et al., 2014).

Ferroptosis is a form of cell death with unique morphological, bioenergetic and genetical features (Freedman A.J.P. et al., 2019 a and b). Unlike autophagy and apoptosis, ferroptosis is an iron- and ROS-dependent cell death characterized by changes in mitochondria cristae and damage of mitochondrial membrane (Yagoda N. et al., 2007; Xie Y. et al., 2016). These cell alterations are due to the loss of selective plasma membrane permeability consequent to the severe membrane lipid peroxidation and iron-induced oxidative stress (Yang W.S. et al., 2016).

In fact, ferroptosis is primarily dependent on the requirement of iron (Fig. 17). In this regard, it has been shown that transferrin, which binds free ferric iron (Fe^{3+}) and transports it into cells, can regulate this type of cell death (Gao M. et al., 2015). Crucial for ferroptosis induction is the accumulation of membrane lipid peroxides spontaneously produced in presence of hydroxyl radicals ($HO^{\cdot}$) generated by iron dependent-Fenton reactions. $HO^{\cdot}$ can react directly with the membrane polyunsaturated fatty acids (PUFAs) triggering a peroxidative chain reaction. PUFAs are particularly sensitive to lipid peroxidation as they contain highly reactive hydrogen atoms within methylene bridges (Halliwell B. et al., 2015).

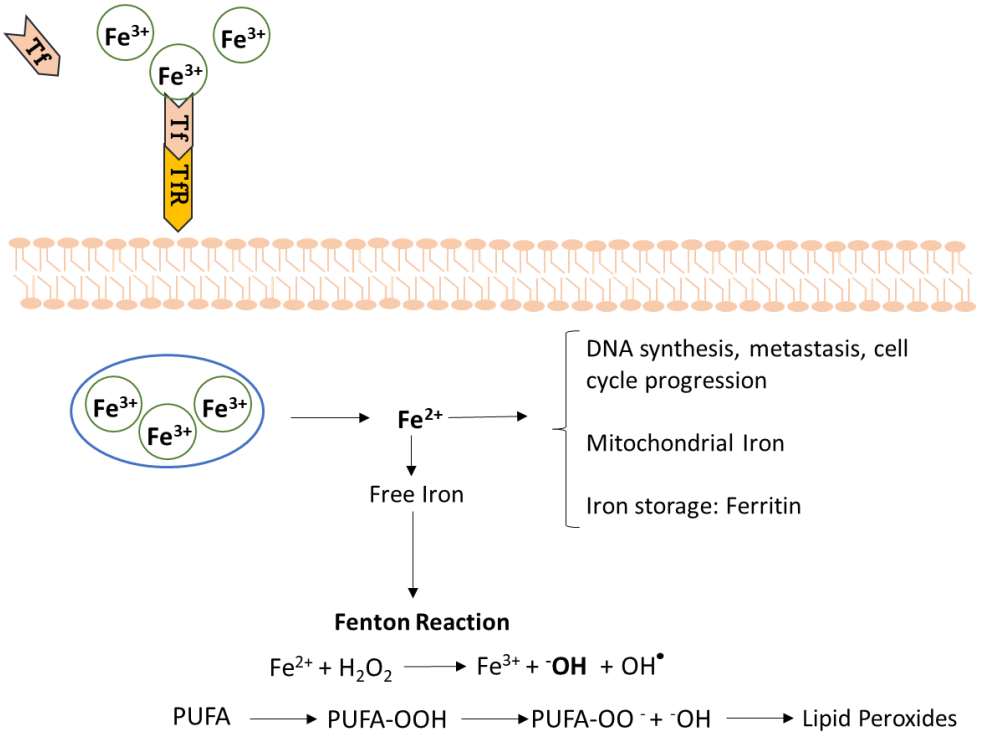

Figure 17. Alterations of iron metabolism and lipid peroxides accumulation.

The metabolism of cysteine is closely related to ferroptosis since it is the limiting factor for GSH biosynthesis: in fact, a dysfunction in cysteine metabolism leads to depletion of intracellular GSH, which serves as a reducing co-substrate for GPX4, the sole enzyme responsible for the repair of oxidized phospholipids. As a consequence of GPX4 inactivation, oxidized phospholipids accumulate leading cell to death (Ursini F. and Maiorino M., 2020). Moreover *in vitro* studies have demonstrated that sensitivity to ferroptosis is dependent on the expression of acyl- CoA synthetase long chain family member 4 (ACSL4), the enzyme catalyzing esterification of PUFA to acyl- CoA (Doll S. et al., 2017; Dixon S.J. et al., 2015).

In this regard, it has been demonstrated that the expression of ACSL4 was related with an aggressive cancer phenotype and it seems to be a predictive marker

for the sensitivity to ferroptosis (Orlando U.D. et al., 2015; Monaco M.E. et al., 2010).

Recent studies have found an anti-ferroptotic gene: the “flavoprotein mitochondria associated apoptosis induction factor 2 (AIFM2)”, whose name has been changed to “ferroptosis suppressor protein 1” (FSP1). FSP1 functions as a NADPH-dependent coenzyme Q (CoQ) oxidoreductase. The reduced form of CoQ, ubiquinol, can act as a radical-trapping antioxidant to prevent lipid peroxidation (Liang D. et al., 2020).

Thus FSP1/CoQ10/NAD(P)H exists as an autonomous parallel system, which can cooperate with GPX4 and GSH to suppress phospholipid peroxidation and, consequently, ferroptosis (Doll S. et al., 2019).

The two main inducers of ferroptosis used *in vitro*, RSL3 (GPX4 inhibitor) and erastin (xCT inhibitor), have poor water solubility and metabolism and consequently their *in vivo* application is problematic (Yang W.S. et al., 2014; Zhang Y. et al., 2019).

Notably, GPX4 inhibitors have been found to induce ferroptosis of cancer stem cells overcoming drug resistance (Fig. 18) (Viswanathan V.S. et al., 2017; Tao Xu et al., 2019).

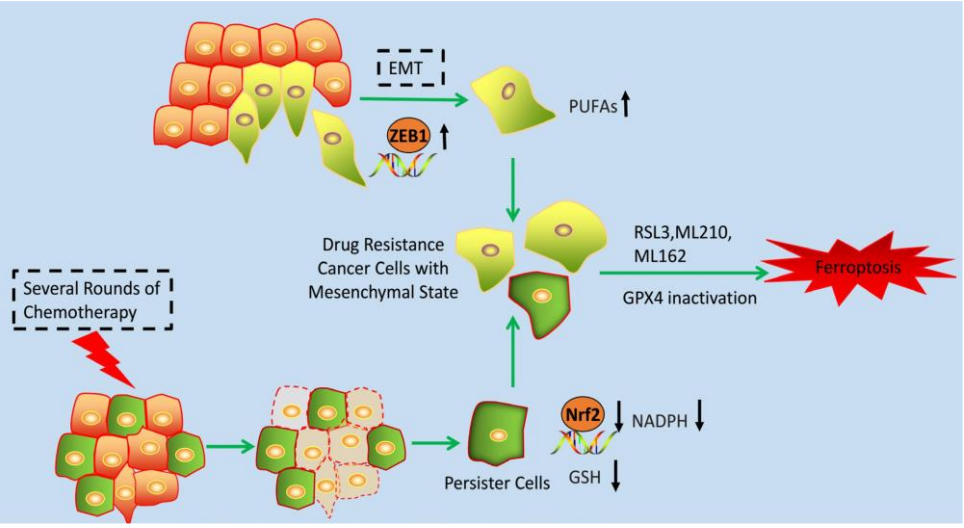

Figure 18. Potential application of ferroptosis inducers to overcome chemoresistance in cancer stem cells. Cancer stem cells survived to several cycles of chemotherapy achieved mesenchymal characteristics, had downregulated Nrf2 target genes and reduced NADPH and GSH levels. GPX4 inactivation triggers ferroptosis of cancer cells with mesenchymal state (Tao Xu et al., 2019).

6. AIM

Several studies demonstrate that tumor cells, compared to their healthy counterparts, have elevated levels of ROS as a consequence of changes in redox homeostasis due to oncogenes, metabolic alterations and mitochondrial dysfunctions (Marengo B. et al., 2016).

Ionizing radiation and chemotherapeutic agents are widely used in the anticancer therapy because they are able to determine the collapse of cellular antioxidant systems by inducing oxidative cell death (Trachootham D. et al., 2009).

However, this approach is not always satisfactory because many primary tumors adapt to the pro-oxidant therapy by overexpressing cellular antioxidants and inducing a state of resistance.

In this regard, it has been shown that the increased expression of antioxidant molecules such as GSH and/or alterations in cellular oxidative metabolism are among the most responsible mechanisms for this redox adaptation (Trachootham D. et al., 2008).

In this context, our previous studies have demonstrated that the acquisition of resistance to Etoposide and doxorubicin is due to the presence of high levels of GSH in resistant neuroblastoma cells and also to their ability to maintain an efficient oxidative metabolism (Colla R. et al., 2016).

Chemoresistance is the primary cause of anti-cancer therapy failure and, as reported in the introduction of the thesis, is also due to the presence of cancer stem cells (CSCs).

CSCs are characterized by low levels of ROS and high antioxidant defenses in comparison to differentiated cancer cells. Their redox state is due to their ability

to synthesize high amounts of GSH by over-expressing xCT, the membrane transporter of cystine (Diehn M. et al., 2009). Furthermore, it has also been found that CSCs are characterized by high levels of CD44 (Yan Y. et al., 2015), a well-known stemness marker that is capable to stabilize xCT in membrane (Ishimoto T. et al., 2011) and whose expression is modulated by PKCα (Nagano O. et al., 2004). Taking into account all these considerations, anticancer research should be focused on discovering innovative approaches able to limit GSH availability in CSCs.

In this context, it has been demonstrated that GSH is fundamental for GPX4 activity that protects cells from the induction of ferroptosis, a form of regulated cell death. Therefore, some strategies finalized to induce ferroptosis could be helpful to overcome drug resistance. In this regard, the two main inducers of ferroptosis used *in vitro*, RSL3 and erastin, cannot be used *in vivo* due to their poor water solubility and metabolism (Yang W.S. et al., 2014; Zhang Y. et al., 2019). Moreover, several drugs capable of inducing ferroptosis have been approved by the Food and Drug Administration (FDA) and among them Sulfasalazine (SSZ, an x-CT inhibitor) has given promising results. However, since SSZ has a short half-life, it is crucial to find more specific and potent xCT inhibitors with a greater bioavailability.

Therefore, in order to investigate new therapeutic approaches, both Etoposide-sensitive and Etoposide-resistant CSCs were long-term treated with Etoposide, alone or in combination with SSZ, or with an inhibitor of the PKCα-dependent pathway (C2-4, a peptide inhibitor), which can target xCT directly or indirectly, respectively.

7. Materials and Methods

7.1 Chemical substances

Etoposide was purchased from Calbiochem (Merk KGaA, Darmstadt, Germany) and sulfasalazine (SSZ), xCT inhibitor, and C2-4, the peptide inhibitor of PKCα, from Cayman Chemical (Ann Arbor, MI, United States). The stock solutions of these compounds were prepared by using dimethylsulfoxide (DMSO) as solvent.

7.2 Generation and maintenance of Cancer Stem Cells (CSCs)

To select neurospheres (Fig. 19; 3D cultures), floating parental cells derived from 2D cultures of HTLA-230 and HTLA-ER (Colla R. et al., 2016) cells were harvested, centrifuged (117 rcf for 8 min), seeded ($16x10^4$) and grown in DMEM-F12 Knock-out (Life Technologies, Carlsbad, CA, USA) containing 1% penicillin/streptomycin (Euroclone S.p.A., Pavia, Italy), 2% B27 (Life Technologies), 40 ng/mL basal growth factor for fibroblasts (bFGF) (R&D Systems, Inc., Minneapolis, MN, USA) and 20 ng/mL epidermal growth factor (EGF) (Life Technologies) (Toma J.G. et al., 2005). It is important to outline that the expression of stem cell markers was evaluated in order to verify the staminality and, only after this characterization, the neurospheres were named as CSCs. HTLA-CSCs and ER-CSCs were split once a week to favor their propagation and, at each passage, the culture medium consisted of 50% fresh medium and 50% of the medium in which the cells were grown (Toma J.G. et al., 2005). In order to analyze CSC propagation, CSCs were collected at any split, centrifuged, mechanically dissociated in PBS and then counted by using a Burker chamber (Marienfeld, Germany).

Parental HTLA-230 and HTLA-ER cells were maintained in RPMI 1640 medium (Euroclone) containing 10% fetal bovine serum (FBS; Euroclone), 2 mM glutamine (Euroclone), 1% penicillin/streptomycin (Euroclone), 1% sodium pyruvate and 2% amino acid solution (Sigma-Aldrich, St. Louis, MO, USA). All cells were periodically tested for the evaluation of any mycoplasma contamination by a semi-quantitative PCR (Mycoplasma Reagent Set; Euroclone).

HTLA-230, a MYCN-amplified stage-IV human neuroblastoma cell line, similar to metastatic bone marrow-isolated NB cells (Castriconi R. et al., 2007), was provided by Dr. L. Raffaghello (G. Gaslini Institute, Genoa, Italy). Cytogenetic features of HTLA-230, including 4p MYCN amplification, del(11)t(11;Y), balanced translocation t(1;17)(p36;q21) and dup(11p) have been described in (Pezzolo et al., 2007).

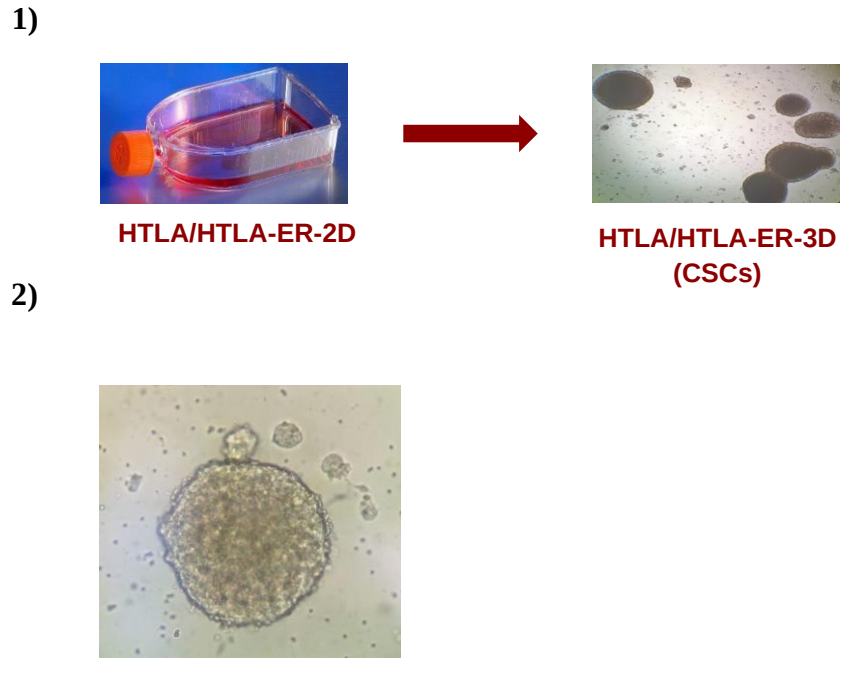

Figure 19. Preparation and maintenance of CSCs in culture. 1) The adherent cells (HTLA and HTLA-ER) were maintained in culture under adequate conditions for the selection of respective neurospheres (3D); 2) photograph of a neurosphere obtained by optical microscope analysis (20x magnification).

7.3 Treatments

CSCs obtained from HTLA-230 and HTLA-ER were treated once a week with 1 mM BSO or three times a week with 0.1 µM C2-4 or with 5 µM SSZ; 1.25 µM Etoposide was administered once a week alone or in combination with C2-4 or SSZ (Fig. 20). The stock solutions of Etoposide, C2-4 and SSZ were prepared in DMSO at the respective concentrations of 50 mM, 1 mM and 50 mM and stored at -20°C. At the time of administration, the compounds were diluted in culture medium to obtain the final concentrations. In order to demonstrate that the doses of DMSO used to dissolve the compounds did not alter the analyses, pilot studies were performed in parallel with the experiments.

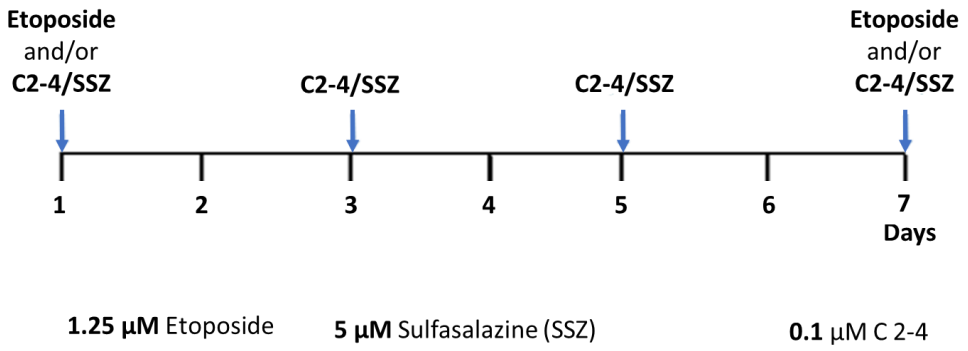

Figure 20. Plan of treatments carried out for six weeks on HTLA and HTLA-ER CSCs.

7.4 Immunofluorescence and Cytofluorimetric Analysis

In order to investigate the expression of CD44, Oct3/4, CD44v9, xCT and vimentin (used as a control of cell permeabilization), cells were analyzed by flow cytometry. In detail, both untreated CSC populations were collected, centrifuged (117 rcf. for 8 min) and then re-suspended in the TrypLE ™ Express Enzyme 1X solution (Invitrogen, Carlsbad, CA, USA). After monitoring CSC disaggregation by microscope analysis, cells were diluted in PBS (137 mM NaCl, 2.6 mM KCl,

10 mM Na_2HPO_4, 1.8 mM KH_2PO_4, pH 7.4). For intracellular staining, prior to incubation with primary mAbs, cells were permeabilized and fixed for 30 min at 4°C with the BD Cytofix/Cytoperm™kit (BD Biosciences, Franklin Lakes, NJ, USA). After this step, CSCs were resuspended in 1% PBS/Saponin solution (Sigma-Aldrich, Milan, Italy) and then centrifuged (365 rcf. for 10 min). Subsequently, CSCs were incubated for 30 min at 4°C with primary antibodies: rabbit polyclonal anti-CD44 (Cosmo Bio, Tokio, Japan), rat monoclonal anti-Oct3/4 (EM92, PE-linked; eBioscience, San Diego, CA, USA), rat monoclonal anti-CD44v9 (RV3, Cosmo Bio), rabbit polyclonal anti-xCT (H-121, Santa Cruz Biotechnology, Dallas, TX, USA) and mouse monoclonal anti-vimentin (V9, Santa Cruz Biotechnology). Labelled cells were then washed with 2% FBS solution in PBS and incubated for 30 min at 4°C with the appropriate isotype-matched secondary antibodies: goat anti-rabbit- IgG-PE (Southern Biotech, Birmingham, AL, USA), goat anti-rat-IgG-FITC (Sigma-Aldrich), goat anti-mouse-IgG-PE (Southern Biotech). Finally, all the samples were fixed with PBS/1% formaldehyde and analyzed with the FACScalibur flow cytometer (BD Biosciences). Data was analyzed by the CellQuest software (BD Biosciences).

7.5 HPLC Analysis of Intracellular Glutathione Levels

Intracellular levels of GSH and GSSG were assessed by high performance liquid chromatography (HPLC) by using the methods reported by Reed for total GSH (Fariss M.W., 1987) and Asensi for GSSG quantification (Asensi M. et al., 1999). Untreated and treated CSCs (1×10^6 cells) were collected and centrifuged (117 rcf. for 8 min). Then, the pellets were washed in PBS, precipitated with 10% perchloric acid (PCA) and the thiol groups were blocked with iodacetic acid (alkaline pH 8–9, 10 min., room temperature, in the dark). Subsequently, the

analytes were converted to 2,4-dinitrophenyl derivatives by incubating the samples with 1% 1-Fluoro-2,4-dinitrobenzene (FDNB) at 4°C in the dark overnight. The quantitative determination of the derivatized analytes was carried out by HPLC equipped with an NH_2 Spherisorb column and a UV detector set at 365 nm with a flow rate of 1.25 ml/min. The mobile phase was maintained at 80% solution A (80% methanol in water) and 20% solution B (0.5 M sodium acetate in 64% methanol in water) for 5 min., followed by a 10-min-linear gradient to 1% A and 99% B. The chromatography was performed with gradient elution.

In order to evaluate GSSG, the samples were incubated with 20 mM N-ethyl-maleimide (NEM) in PCA and, after precipitation and alkalization of the sample (alkaline pH 8–9, 10 min., room temperature, in the dark), derivatization was carried out by adding 1% FDNB. In order to allow the elution of GSSG, the mobile phase was kept at 99% solution B for a further 15 min.

The data obtained was normalized by the intracellular amount of protein and expressed as Eq/mg of protein.

7.6 ATP Synthesis

The ATP content was measured by using the luciferin/luciferase ATP bioluminescence assay kit CLSII (Roche, Basel, Switzerland) on a Luminometer (Triathler, Bioscan, Washington, DC, USA) (Colla R. et al., 2016). ATP standard solutions (Roche, Basel, Switzerland) in the concentration range of 10^{-10} – 10^{-7} M were used for calibration. The assay was carried out at 37°C over 2 min. by measuring formed ATP from added ADP. Untreated and treated CSCs were incubated for 10 min. with the assay buffer (10 mM Tris-HCl pH 7.4, 50 mM KCl, 1 mM EGTA, 2 mM EDTA, 5 mM KH_2PO_4, 2 mM $MgCl_2$, 0.6 mM Ouabain, 0.040 mg/mL Ampicillin, 0.2 mM di(adenosine-50) penta-phosphate, 0.2 mM and

5 mM pyruvate plus 2.5 mM malate). Afterwards, ATP synthesis was induced by the addition of 0.3 mM ADP.

7.7 Oxygen Consumption Rate (OCR)

In order to measure the respiratory activity, 2 x 10^5 cells were analyzed by using an amperometric electrode for O_2 placed in an isolated chamber and stirring maintained at 37°C (Colla R. et al., 2016). Untreated and treated CSCs were collected and centrifuged (117 rcf. for 8 min.). Then, the pellets were suspended in the assay buffer (137 mM NaCl, 5 mM KH_2PO_4, 5 mM KCl, 0.5 mM EDTA, 3 mM $MgCl_2$ and 25 mM Tris–HCl, pH 7.4) and permeabilized with 0.3% digitonin for 10 min. Then, the sample was transferred to the chamber; to measure the maximum respiration rate, 5 mM pyruvate and 2.5 mM malate were added.

7.8 Glucose Consumption

Glucose consumption was assessed by measuring its concentration with a double beam spectrophotometer (UNICAM UV2, Analytical S.n.c., Langhirano, PR, Italy), by using the hexokinase (HK) and glucose 6 phosphate dehydrogenase (G6PD) coupling system, following NADP reduction at 340 nm (Colla R. et al., 2016). The buffer assay was composed of 100 mM Tris HCl, pH 7.4, 2 mM ATP, 10 mM NADP, 2 mM $MgCl_2$, 2 IU of HK and 2 IU of G6PD. The reaction was started after the addition of 5 µl of CSC medium.

7.9 Lactate Release

The concentration of lactic acid released by CSCs in the culture medium was analyzed by spectrophotometric analysis (Colla R. et al., 2016). The assay buffer was composed of 100 mM Tris/HCl (pH 8), 5 mM NAD^+ and 1 IU/mL of lactate

dehydrogenase. Samples were analyzed before and after the addition of 4 µg of purified lactate dehydrogenase.

7.10 MDA Production

Malondialdehyde (MDA) levels were analyzed by thiobarbituric acid assay (TBARS) (Colla R. et al., 2016; Ravera S. et al., 2015). Briefly, 50 µg of total proteins, derived from each sample, were dissolved in 300 µl of Milli-Q water and added to 600 µl of TBARS solution containing 15% trichloroacetic acid (TCA) and 26 mM thiobarbituric acid (TBA) in 0.25 N HCl. This mixture was incubated for 40 min. at 100°C and then centrifuged (20,800 rcf.for 2 min).

Subsequently, the supernatant was collected and analyzed by spectrophotometer at 532 nm wavelength. In order to calculate MDA concentration, the absorbance of each sample was compared with that obtained from a standard curve evaluated with known concentrations of MDA (0.75, 1 and 2 µM).

7.11 ROS Production

Detection of ROS levels was evaluated by incubating CSCs with 5 µM 2'-7' di-chlorofluorescein-diacetate (DCFH-DA; Sigma-Aldrich) (Colla R. et al., 2016). Then, the accumulation of dichlorofluorescein (DCF) was analyzed by flow cytometry by using a FACSCanto II flo cytometer (BD) using FlowJo (Tree Star, Inc). At least 10,000 events were analyzed.

7.12 Total protein extraction

At the end of the treatments, cells were pelleted by centrifugation (800 rpm for 8 min. at 8°C) and resuspended in lysis buffer (50 mM Tris Hcl, 150 mM NaCl,

2 mM EDTA, 1 mM EGTA, 50 mM EGF, 1 mM PMSF) containing a mixture of 7X protease inhibitors (complete Mini Protease, Roche) and 1% Triton X-100 (Sigma). The cell suspension, which was further lysed by passing it 10 times through a 25 Gauge needle equipped syringe, was then centrifuged (15'000 g for 10 min. at 8°C; Heraeus Centrifuge Biofuge 28RS). The supernatant containing the total proteins was collected and stored at - 80°C.

7.13 Total protein assay

The amount of total proteins was determined by using PierceTM BCA Protein Assay Kit (Thermo Scientific). This assay measures the reduction of Cu^{2+} to Cu^{+} in an alkaline solution through the Biuret reaction using the bicinconic acid (BCA) containing reagent. Under alkaline conditions, BCA is a highly sensitive, stable and specific reagent for Cu^{+}. The purple color of the product is due to the chelation of 2 BCA molecules with one of Cu^{+}, whose intensity is proportional to the amount of proteins.

The macromolecular structure of proteins, the number of peptide bonds and the presence of particular amino acids (cysteine, tyrosine, tryptophan and cystine) are responsible for the color formation with the BCA. The change in the intensity is determined by spectrophotometer analysis. The test was carried out on a 96-well plate in which samples and standards were incubated at 37°C x 30 min. and then analyzed by spectrophotometer at 570 nm wavelenght (BioRad iMark plate reader).

Total protein amounts of the samples were calculated respect to a calibration straight line obtained by using bovine serum albumin (BSA) at known concentrations (mg/mL) as a standard.

7.14 Western Blot Analyses

Protein aliquots (25 μg) were mixed with 3.5x loading dye (62.5 mM Tris-HCl, pH 6.8, 2% SDS, 25% glycerol, 0.01% bromophenol blue, 62.5 mM β-mercapto-ethanol) and denatured at 100°C x 5 min. and subjected to electrophoresis by using 4-20 % Mini-PROTEAN TGX ™ Precast Gels (Biorad) along with protein marker (Sharpmass VII, Euroclone). At the end of the electrophoretic run, the proteins were transferred by electroblotting onto Hybond P 0.45 PVDF membrane (Polyvinylidene fluoride, GE Healthcare Amersham) which was subsequently colored with a solution of Ponceau red in order to verify the transfer.

Non-specific binding sites were blocked by incubating membrane with 5% dry non-fat milk in PBS-Tween (80 mM Na_2PO_4, 20 mM NaH_2PO_4, 100 mM NaCl, 0.1% Tween 20) for 1 hr at room temeperature. Then, membranes were incubated overnight by using rabbit antibody anti-N-Cadherin (D4R1H), anti-ZEB-1 (D80D3), anti-Vimentin (D21H3), anti-β Catenin (D10A8), anti-Claudin-1 (D5H1D) (Cell Signaling Technology Inc., Danvers, MA, USA Upstate, Lake Placid, NY, USA) and anti-GPX4 (Abcam, Cambridge, UK). Membranes were washed 3x in TBS-Tween (20 mM Trizma base, 0.5 M NaCl, 0.1% Tween 20) and then incubated for 1 hr with the suitable HRP-conjugated secondary antibody (GeHealthcare, Buckingamshire UK). The signal was detected using ECL chemiluminescence system detection kit (Pierce™ ECL Western Blotting Substrate, ThermoFisher) and analysed with an image densitometer connected to Quantity One Software (Bio-Rad Laboratories, Hercules, CA, USA).

7.15 GPX4 Activity Assay

GPX4 activity was evaluated by standard methods (Roveri A. et al., 1994). Cell pellets were resuspended in 0.75 ml lysis buffer (0.1 M Tris-HCl, 0.25 M sucrose, protease inhibitors, pH 7.5) and then sonicated and used in the test (0.1-0.2 ml of sample per test). Samples were mixed with the assay buffer (0.1 M Tris-HCl pH 7.8, 5 mM EDTA, 5 mM GSH, 0.1% (v/v) Triton X-100, 0.16 mM NADPH and 0.6 IU/ml Glutathione Reductase). The sample was incubated for 5 min at 25°C, then the baseline was recorded at 340 nm for about 1 min and finally the enzymatic activity was started by adding 0.020 mM phosphatidylcholine hydroperoxide (PCOOH) and quantified as the decrease of absorbance at 340 nm due to $NADPH^{+}$ oxidation by Glutathione Reductase, as reported by Roveri (Roveri et al., 1994). GPX4-specific activity was expressed as nmoles/min/mg.

7.16 Principal Component Analyses (PCA)

PCA is a data display method for multivariate analysis. Given a data set in which each sample is described by n variables, PCA aims to find new directions, linear combinations of the original ones (Leardi R., 2018). The first component (PC1) corresponds to the direction explaining the maximum variance, while PC2 is the direction, orthogonal to PC1, explaining the maximum variance not explained by PC1, and so on. The result is that a limited number of components is sufficient to explain the relevant part of the information.

The loadings are the coefficients of the linear combinations corresponding to the PCs. By plotting them in a loading plot it is possible to understand the relationships among the variables in the multivariate space. On the other side, the score plot allows visualization of the location of the samples in the space described by the PCs, hence making possible to check similarities and differences among

the samples. The elaborations and the plots were carried out by using CAT software (Leardi R. et al., software).

7.17 Statistical analysis

The results were expressed as mean value ± SEM and derive from the data obtained from 4 independent experiments. The statistical significance was assessed by one-way ANOVA analysis followed by the Dunnet test for the multiple comparison of the results.

8. Results

8.1. Neurospheres, isolated from parental HTLA-230 and HTLA-ER cells, express stemness markers

In order to verify if the selected neurospheres, isolated from floating HTLA-230 and HTLA-ER cells (Colla R. et al., 2016), were formed by stem cells, the expression of CD44 and Oct-3/4, known markers of stemness, was analyzed. As shown in Figure 21, selected neurospheres expressed CD44 and Oct-3/4, demonstrating that both cell populations have staminality characteristics and, consequently, they have been named as HTLA- and ER-cancer stem cells (HTLA-CSCs and ER-CSCs).

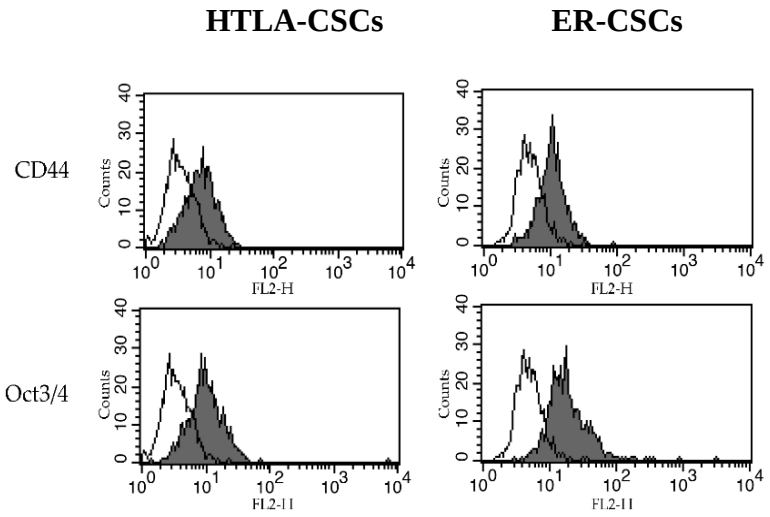

Figure 21. Selected neurospheres isolated from HTLA and HTLA-ER cells express CD44 and Oct3/4 staminality markers. Flow cytometric analysis of CD44 and Oct3/4 expression in untreated HTLA-CSCs and ER-CSCs. Cells were permeabilized, stained with mAbs against CD44 or Oct3/4 and analyzed by flow cytometry. Grey profiles indicate cells stained with the different mAbs, while white profiles correspond to isotype control. One representative experiment of five is shown.

8.2. GSH plays a crucial role in the formation and maintenance of CSCs and its depletion efficiently counteracts CSC chemoresistance

Our previous study demonstrated that the high intracellular GSH levels play a crucial role in chemoresistance (Colla R. et al., 2016) and taking into account that therapy failure is also dependent on the presence of CSCs, the relationship between GSH levels and CSCs was investigated. Therefore, both CSC populations were treated once a week for 6 weeks with 1 mM BSO, a known GSH-depleting compound (Galluzzi L. et al., 2012; Helleday T. et al., 2010); as shown in Figure 22, 2-week BSO exposure was able to counteract the formation of HTLA-CSCs, while in ER-CSCs a similar effect was observed only after 5 weeks.

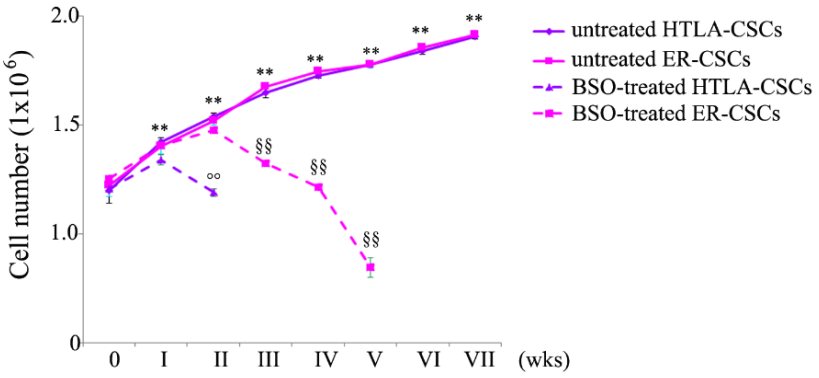

Figure 22. Chronic BSO treatment counteracts CSC formation at different times in HTLA and ER-CSC. Both CSC populations were treated (once a week for 6 weeks) with 1 mM BSO and, at any split, disaggregated CSCs were counted by using a Burker chamber as described in Materials and Methods. **p<0.01 vs. time 0; °°p<0.01 vs. untreated HTLA-CSCs; §§p<0.01 vs. untreated ER-CSCs.

Although BSO has been found to counteract CSC formation, both *in vitro* and *in vivo* (Miran T. et al., 2018; Boivin A. et al., 2011) and has been included in clinical trials (Villablanca J.G. et al., 2016), its therapeutic use is limited by its short half-life and non-selective depleting effects on cancer cells (Matsushima H. et al., 1992).

In order to overcome this limitation, an effective strategy could be the indirect modulation of GSH levels by acting on GSH-related targets. In this context, it has been reported that CD44v9, a variant of CD44, contributes to the stabilization of xCT on cell membrane, by favoring the uptake of cystine, the essential aminoacid for GSH biosynthesis. Considering that the expression of CD44 is modulated by PKC-α (Nagano O. et al., 2004; Okamoto et al., 1999), a potential strategy would be to reduce the CD44 expression by inhibiting this kinase. As shown in Figure 23, both CSC populations expressed CD44v9 and xCT, thus justifying the use of C2-4, a PKCα inhibitor, or SSZ, a xCT inhibitor in the present study.

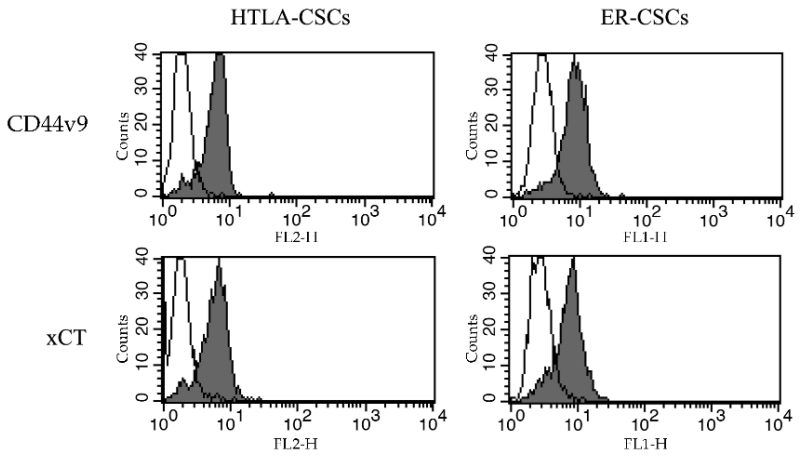

Figure 23. Both CSC populations express CD44v9 and xCT. Cells were permeabilized, stained with mAbs to the indicated molecules, and analyzed by flow cytometry. Grey profiles indicate cells stained with the different mAbs, while white profiles correspond to isotype control. One representative experiment of five is shown.

8.3. Etoposide prevents HTLA-CSC formation after 3 weeks while counteracts the fomation of ER-CSC when it is combined with SSZ or C2-4 for 6 weeks

As shown in Figure 24, Etoposide reduced the formation of HTLA-CSCs by 35% after only 1 week of exposure and totally prevented CSCs formation after 3 weeks (Fig. 24a). Moreover, similar results were obtained in CSCs co-treated with either Etoposide and SSZ (Fig. 24a, left panel) or Etoposide and C2-4 (Fig. 24a, right panel). However, treatments with SSZ (Fig. 24a, left panel) or C2-4 alone (Fig. 24a, right panel) did not significantly change this parameter during the analyzed time points.

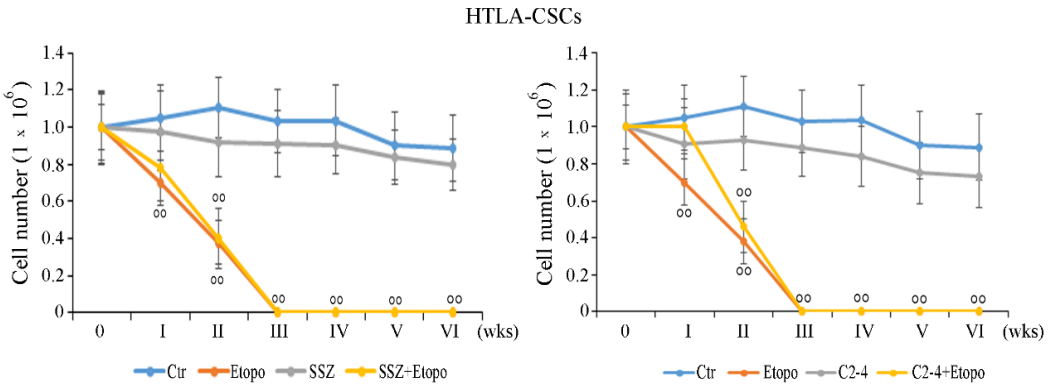

Figure 24. Evaluation of cell number in HTLA-CSCs treated three times a week with 0.1 μM C2-4, with 5 μM SSZ or with 1.25 μM Etoposide, administered once a week alone or in combination with C2-4 or SSZ. The treatments were protracted for 6 weeks. In order to evaluate CSCs propagation, at any split, disaggregated CSCs were counted by using a Burker chamber as described in Materials and Methods. °°$p<0.01$ vs. untreated HTLA-CSCs (Ctr); *$p<0.05$ vs. untreated ER-CSCs (Ctr); ##$p<0.01$ vs. Etoposide-treated ER-CSCs.

The analysis of the same paramether in ER-CSCs showed that the same treatments did not induce any significant alteration until 2 weeks of exposure (Fig. 25). In fact, 4 weeks of Etoposide exposure reduced ER-CSC formation by 38% and this effect remained unchanged until 6 weeks (Fig. 25). Interestingly, it has been observed that Etoposide combined with SSZ or C 2-4 reduced ER-CSC propagation by 30% and 55% respectively after 3 weeks, and totally prevented the formation of CSCs after 6 weeks (Fig. 25). In addition, in ER-CSCs, the treatment with SSZ alone for 6 weeks gave similar results to those observed in Etoposide-treated cells, while C2-4 *per se* did not influence CSC formation and propagation (Fig. 25, right panel).

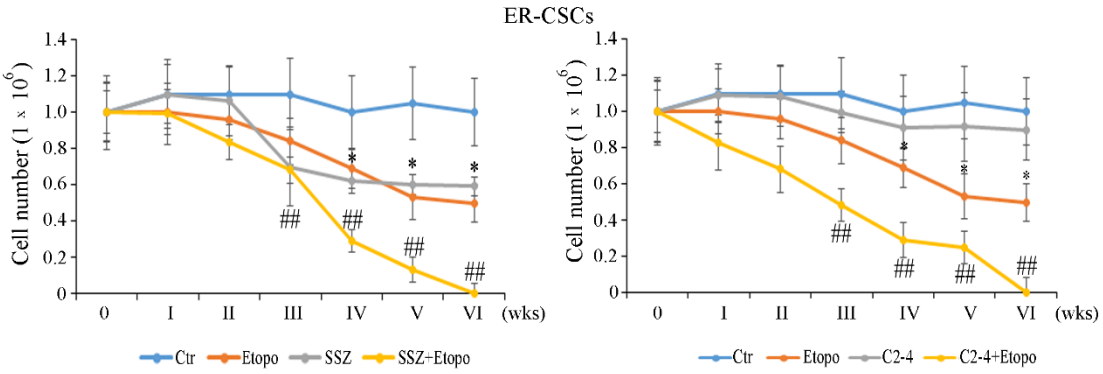

Figure 25. Evaluation of cell number in ER-CSCs treated three times a week with 0.1 μM C2-4, with 5 μM SSZ or with 1.25 μM Etoposide, administered once a week alone or in combination with C2-4 or SSZ. The treatments were protracted for 6 weeks. In order to evaluate CSC propagation, at any split, disaggregated CSCs were counted by using a Burker chamber as described in Materials and Methods. °°$p<0.01$ vs. untreated HTLA-CSCs (Ctr); *$p<0.05$ vs. untreated ER-CSCs (Ctr); ##$p<0.01$ vs. Etoposide-treated ER-CSCs.

Given that the formation of HTLA-CSCs was totally inhibited after 3 weeks of treatments and that of ER-CSCs after 6 weeks, the following analyses were performed after 2 and 5 weeks respectively.

8.4. Etoposide induces a marked depletion of GSH in HTLA-CSCs after 2 weeks while the same effect is not observed in ER-CSCs until 5 weeks of treatment

As shown in Fig. 26, untreated HTLA-CSCs and ER-CSCs had comparable GSH levels (about 17.07 μEq/g and 17.37 μEq/g proteins, respectively). After 2-week Etoposide exposure, GSH levels were reduced by 80% in HTLA-CSCs with respect to untreated CSCs (Fig, 26a); both co-treatment conditions (C2-4+Etoposide or SSZ+Etoposide) exerted similar effects to those observed in Etoposide treated CSCs (Fig. 26a), while the treatment with C2-4 or SSZ alone did not change the GSH amount (Fig. 26a). The same 2 week-treatments in ER-CSCs did not induce any significant changes in GSH levels (Fig. 26b). After 5 weeks, untreated ER-CSCs displayed a major amount of GSH (8.99 μE/g proteins) in comparison with HTLA-CSCs (4.7 μE/g proteins). Since 5 week-treatment with Etoposide, alone or in combination, totally counteracted HTLA-CSC formation (Fig. 24a), it was not possible to analyze GSH. As shown in Figure 26c, Etoposide reduced GSH of ER-CSCs by 60% in comparison to untreated CSCs and both co-treatments did not change the GSH-depleting effect of Etoposide. The amount of GSSG, the oxidized form of GSH, was below to the detection limits in both CSC populations after 2 weeks while it was depleted by 60-65% in ER-CSCs after the 5 week-treatment with Etoposide, alone or in combination with C2-4 or SSZ (data not shown).

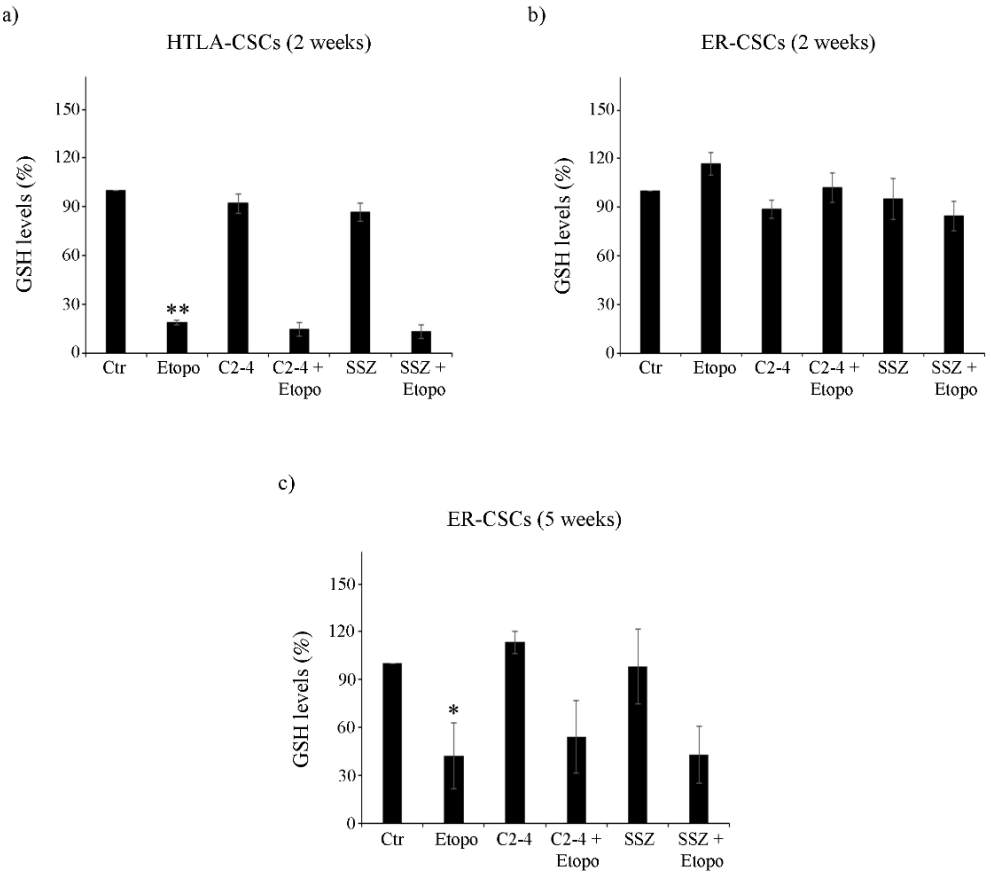

Figure 26. GSH levels in both CSC populations treated for 2 (a, b) or 5 weeks (c). HTLA-CSCs and ER-CSCs were treated three times a week with 0.1 μM C2-4, with 5 μM SSZ or with 1.25 μM Etoposide, administered once a week alone or in combination with C2-4 or SSZ. GSH levels were determined by HPLC analysis and expressed as percentages of the control value. *p<0.05 vs. untreated CSCs (Ctr); **p<0.01 vs. untreated CSCs (Ctr).

The results obtained demonstrate that the survival of Etoposide-resistant CSCs is not totally dependent on GSH since, even though Etoposide exerts a severe GSH-depleting action, it does not totally counteract CSC generation, suggesting that other factors might contribute to the maintenance of cancer stem cell survival.

In this regard, it has been widely demonstrated that cancer cells usually depend on glycolysis for energy production (Backos D.S. et al., 2012; Towsend D.M. et al., 2003; Koppenol W.H. et al., 2011) while chemoresistant cancer cells and

CSCs undergo a metabolic rewiring, stimulating OXPHOS with a major ATP production (Sikalidis A.K. et al., Amino Acids; Ali-Osman F. et al., 1989; Evans C.G. et al., 1987). Therefore, based on these findings, the metabolic profile of CSCs was analyzed.

8.5. ATP synthesis is reduced in HTLA-CSCs after 2 weeks of Etoposide and in ER-CSCs after 5 weeks of co-treatments with SSZ or C2-4

As shown in Figure 27, after 2 weeks, untreated HTLA-CSCs have a double amount of ATP in comparison to ER-CSCs. In HTLA-CSCs, two week-Etoposide, alone or in combination with C2-4 or SSZ, reduced ATP levels by 70% in compared to untreated CSCs (Fig. 27a).

Notably, in ER-CSCs, 2 week-Etoposide combined with SSZ was able to reduce ATP by 25% in respect to untreated and Etoposide-treated CSCs (Fig. 27b). After 5 weeks, both untreated CSC populations had comparable levels of ATP (10 nmol/min/1x10^6 cells). Given that 5 week-Etoposide, alone or in combination with SSZ or C2-4, totally prevented the formation of HTLA-CSCs (Fig. 24), the evaluation of ATP synthesis was not possible. Instead, as shown in Figure 27c, Etoposide reduced ATP levels by 10 % in ER-CSCs, and both co-treatments further decreased ATP by 25% (Figure 27c).

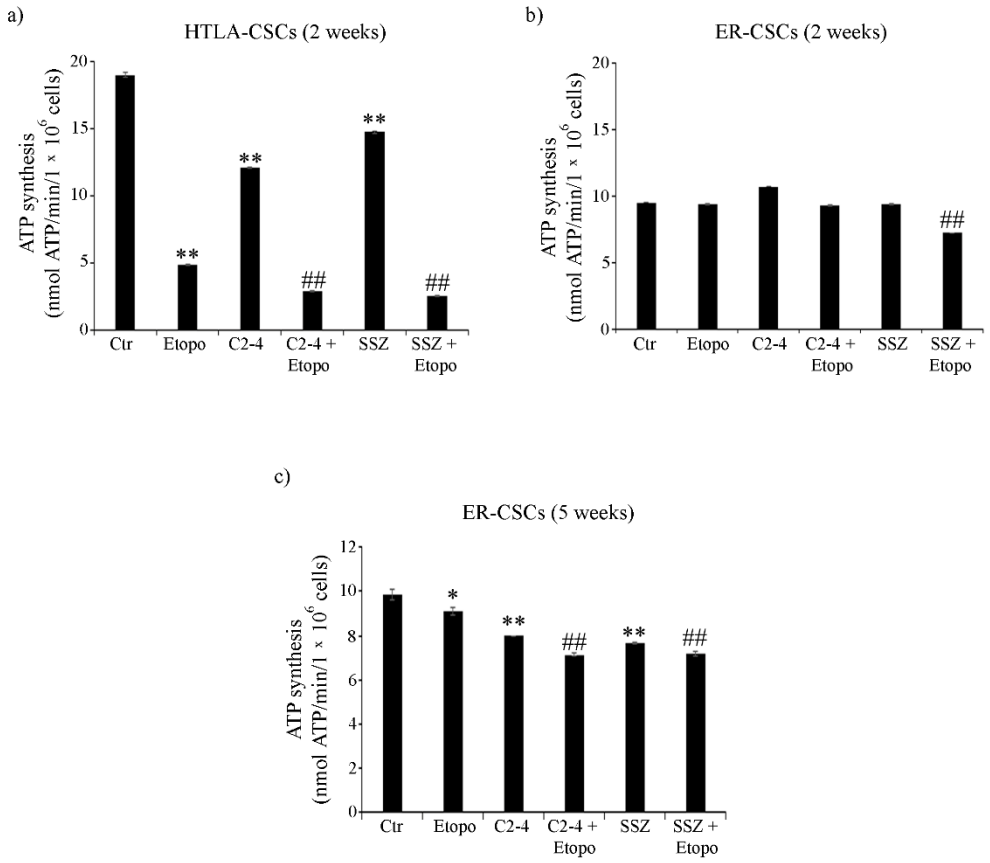

Figure 27. ATP synthesis in both CSC populations treated for 2 (a, b) or 5 weeks (c). HTLA-CSCs and ER-CSCs were treated three times a week with 0.1 μM C2-4, with 5 μM SSZ or with 1.25 μM Etoposide, administered once a week alone or in combination with C2-4 or SSZ. Results were reported as nmol ATP/min/10^6 cells. Bar graph summarizes quantitative data of means ± S.E.M. of three independent experiments. *p<0.05 vs. untreated CSCs (Ctr); **p<0.01 vs. untreated CSCs (Ctr); $^{\#\#}$p<0.01 vs. Etoposide-treated CSCs.

8.6. O_2 consumption in HTLA-CSCs decreases after 2 week-Etoposide alone or in combination with C2-4 or SSZ, while in ER-CSCs is not significantly altered under all treatment conditions

In HTLA-CSCs, 2 week-Etoposide reduced the oxygen consumption rate (OCR) by 75% in respect to untreated CSCs (Fig. 28a) and similar results were observed in co-treated ones (Fig. 28a). In ER-CSCs, 2 week-Etoposide, alone or in combination with inhibitors, did not induce significant alterations of OCR, while a 15% and 35% increase was observed after treatment with SSZ or C2-4 alone respectively (Fig. 28b). Moreover, after 5 weeks, none of the treatments or co-treatments significantly changed the OCR in ER CSCs (Fig. 28c).

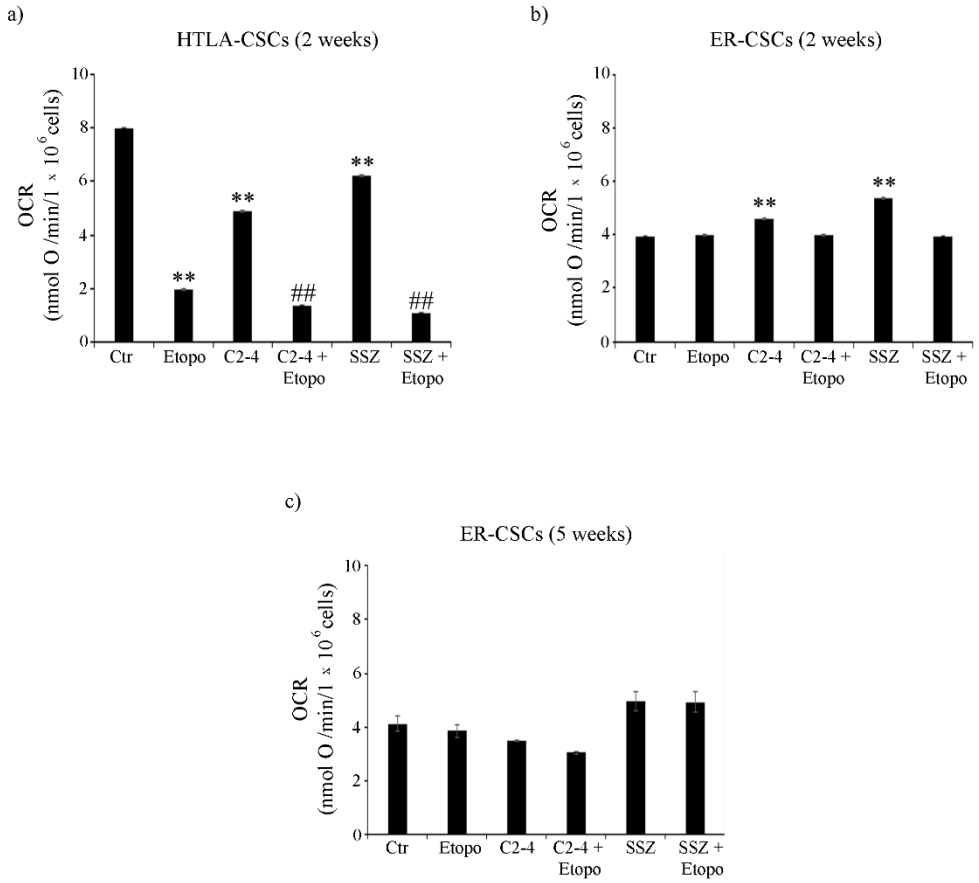

Figure 28. Oxygen consumption rate (OCR) in both CSC populations treated for 2 (a, b) or 5 weeks (c). HTLA-CSCs and ER-CSCs were treated three times a week with 0.1 μM C2-4, with 5 μM SSZ or with 1.25 μM Etoposide, administered once a week alone or in combination with C2-4 or

SSZ. Results were reported as nmol O/min/10^6cells. Bar graph summarizes quantitative data of means ± S.E.M. of three independent experiments. *p<0.05 vs. untreated CSCs (Ctr); **p<0.01 vs. untreated CSCs (Ctr); $^{\#\#}$p<0.01 vs. Etoposide-treated CSCs.

To verify the efficiency of OXPHOS, the P/O value was calculated. In detail, in both CSC populations, the P/O ratio was 2.3 ± 0.2 which is comparable to the physiological level of 2.5 (Hinkle P.C., 2005). Interestingly, only in CSCs treated with SSZ, alone or in combination with Etoposide for 2 or 5 weeks, the P/O value was 1.8±0.15.

8.7. Glucose consumption and lactic acid production by HTLA-CSCs are increased after Etoposide alone or in association with C 2-4 or SSZ. Etoposide and co-treatments lead to an increase of glucose consumption in ER-CSCs while only the co-treatments enhance the lactic acid release in ER-CSCs

In order to complete the analysis of cell metabolism, glucose consumption and lactate release were evaluated under all experimental conditions.As shown in Fig. 29a, untreated HTLA-CSCs consumed about 40% more glucose than untreated ER-CSCs. In HTLA-CSCs, 2 week-Etoposide increased glucose consumption by 60% compared to untreated CSCs and the co-treatments did not modify the Etoposide-induced effect (Fig. 29a). In ER-CSCs, 2 week-treatments with either Etoposide, C2-4 or SSZ increased glucose consumption by 30% as compared to untreated CSCs, and C2-4 or SSZ co-treatments stimulated this parameter by a further 60% and 25%, respectively (Fig. 29b). Since 5 week-treatment with Etoposide, alone or in combination, totally counteracted HTLA-CSC formation (Figure 24a), the analysis of glucose consumption was not possible. Instead in 5-week-treated ER-CSCs the results obtained were similar to those observed after 2

weeks and, also in this case, the presence of SSZ or C2-4 further stimulated the Etoposide-induced effects (Fig. 29c).

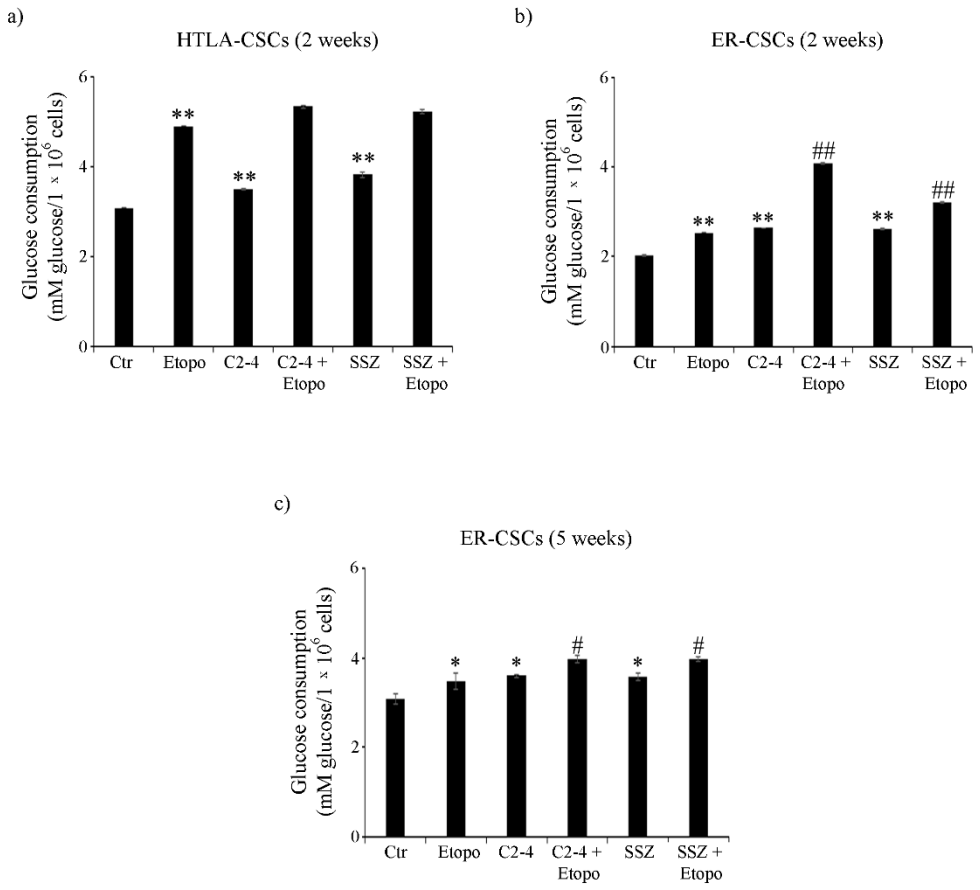

Figure 29. Glucose consumption in both CSC populations treated for 2 (a, b) or 5 weeks (c). HTLA-CSCs and ER-CSCs were treated three times a week with 0.1 μM C2-4, with 5 μM SSZ or with 1.25 μM Etoposide, administered once a week alone or in combination with C2-4 or SSZ. Results were reported as mM glucose/10^6 cells. Bar graph summarizes quantitative data of means ± S.E.M. of three independent experiments. *p<0.05 vs. untreated CSCs (Ctr); **p<0.01 vs. untreated CSCs (Ctr); $^{\#}$p<0.05 vs. Etoposide-treated CSCs; $^{\#\#}$p<0.01 vs. Etoposide-treated CSCs.

The changes in glucose consumption were accompanied by alterations of the lactate release. In fact, in line with the highest level of glucose consumption observed in untreated HTLA-CSCs, an increase of 50% in the lactate release was

detected in comparison with untreated ER-CSCs (Fig. 30a and b). After 2 weeks, the Etoposide exposure of HTLA-CSCs stimulated the lactate release by 80% compared to untreated CSCs, and the co-treatments did not modify the Etoposide-induced effect (Fig. 30a). In ER-CSCs, a similar effect was observed in C2-4 or SSZ-treated or co-treated cells (Fig. 30b). After 5 weeks, both co-treatments stimulated lactate release by 30% in comparison to untreated and treated ER-CSCs (Fig. 30c).

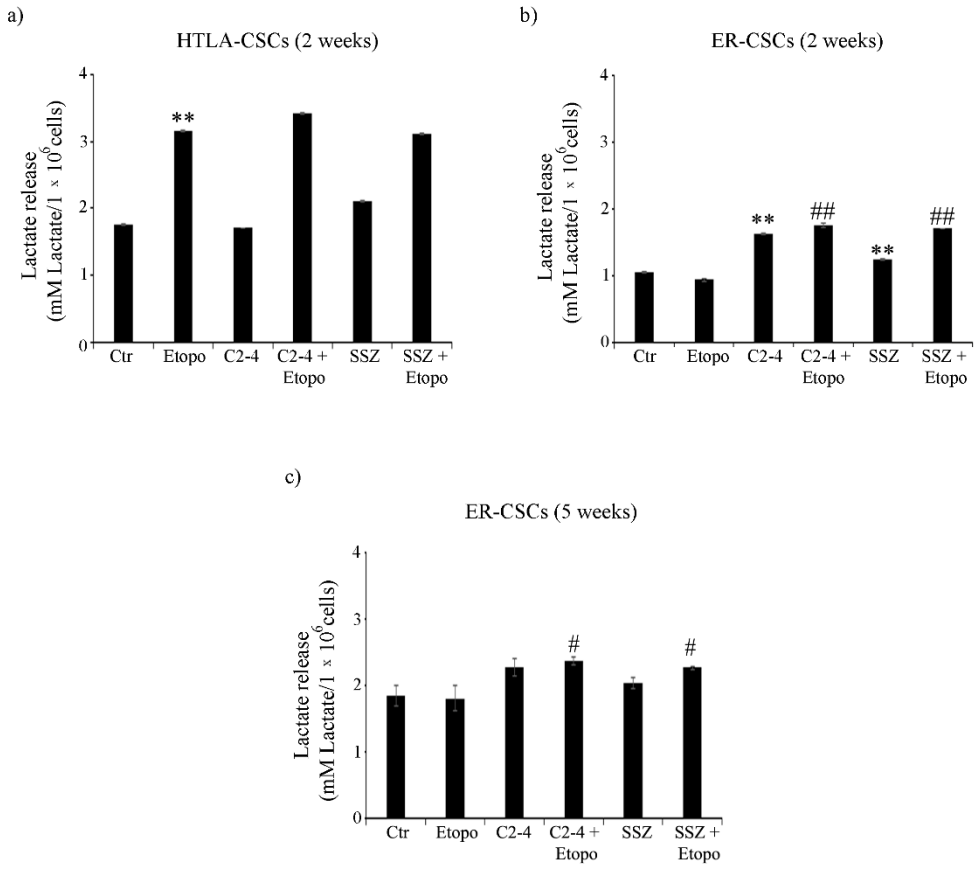

Figure 30. Lactate release in both CSC populations treated for 2 (a, b) or 5 weeks (c). HTLA-CSCs and ER-CSCs were treated three times a week with 0.1 μM C2-4, with 5 μM SSZ or with 1.25 μM Etoposide, administered once a week alone or in combination with C2-4 or SSZ. Results were reported as mM lactate/10^6 cells. Bar graph summarizes quantitative data of means ± S.E.M. of three independent experiments. **$p<0.01$ vs. untreated CSCs (Ctr); $^{\#}p<0.05$ vs. Etoposide-treated CSCs; $^{\#\#}p<0.01$ vs. Etoposide-treated CSCs.

8.8. Etoposide induces lipid peroxidation in HTLA-CSCs that was triggered in ER-CSCs by co-treatments

In order to better characterize cell damage, the production of malondialdehyde (MDA), a marker of membrane lipid peroxidation, was evaluated. As shown in Figure 31a, 2-week treatments of HTLA-CSCs with Etoposide or SSZ alone increased MDA levels by 100% and the co-treatments with SSZ increased this parameter by an additional 30%. In ER-CSCs, only 2-week exposure to SSZ, alone or in combination with Etoposide, stimulated by 85% the production of MDA (Fig. 29b). After 5 weeks, in SSZ treated/co-treated ER-CSCs, MDA levels were similar to those observed after two weeks, while a 35% increase of MDA levels was found in ER-CSCs co-treated with C2-4 (Fig. 31c).

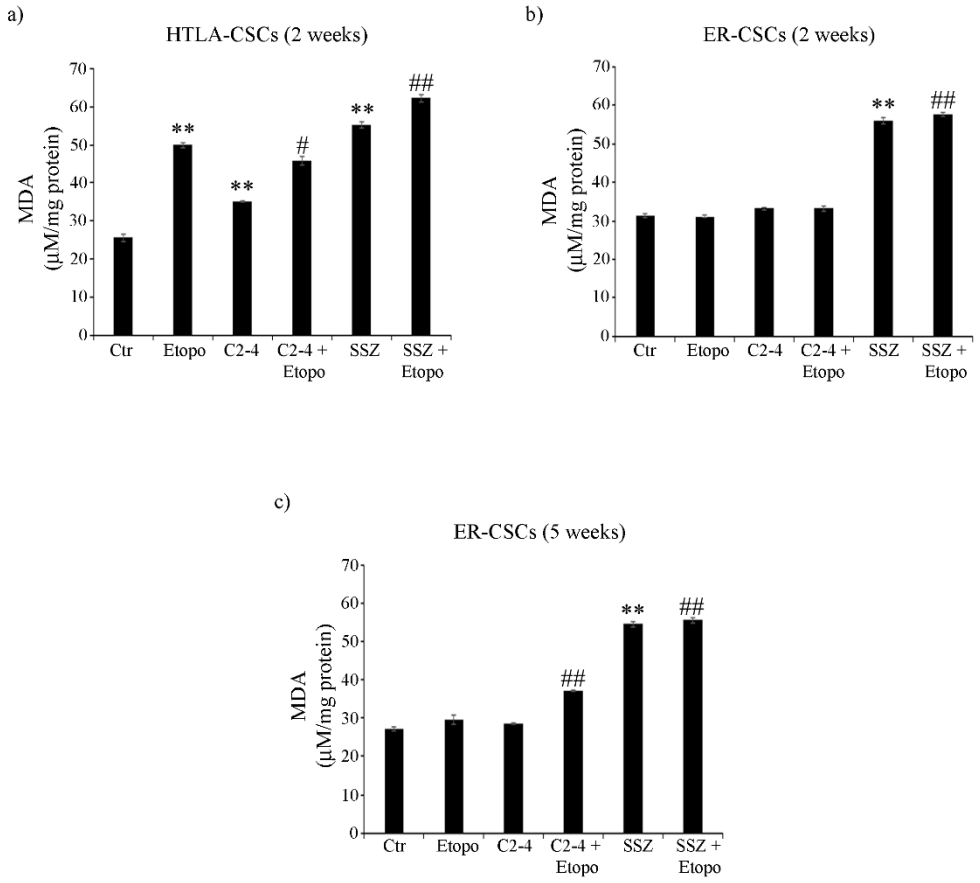

Figure 31. MDA production in both CSC populations treated for 2 (a,b) or 5 weeks (c). HTLA-CSCs and ER-CSCs were treated three times a week with 0.1 μM C2-4, with 5 μM SSZ or with 1.25 μM Etoposide, administered once a week alone or in combination with C2-4 or SSZ. Results were reported as μM/mg protein. Bar graph summarizes quantitative data of means ± S.E.M. of three independent experiments. **$p<0.01$ vs. untreated CSCs (Ctr); $^{\#}p<0.05$ vs. Etoposide-treated CSCs; $^{\#\#}p<0.01$ vs. Etoposide-treated CSCs.

Considering that mitochondrial oxidative phosphorylation can generate ROS, this parameter was evaluated in both CSC populations and under all experimental conditions. As shown in Figure 32a, in HTLA-CSCs none of the treatments or co-treatments induced significant changes in ROS production after 2 weeks. Instead, 2-week treatment of ER-CSCs with Etoposide, alone or in combination with C2-4 or SSZ, induced a 60% reduction in ROS levels compared to untreated ones (Fig. 32b). After 5 weeks of all treatments, no changes in ROS production were detected (Fig. 32c).

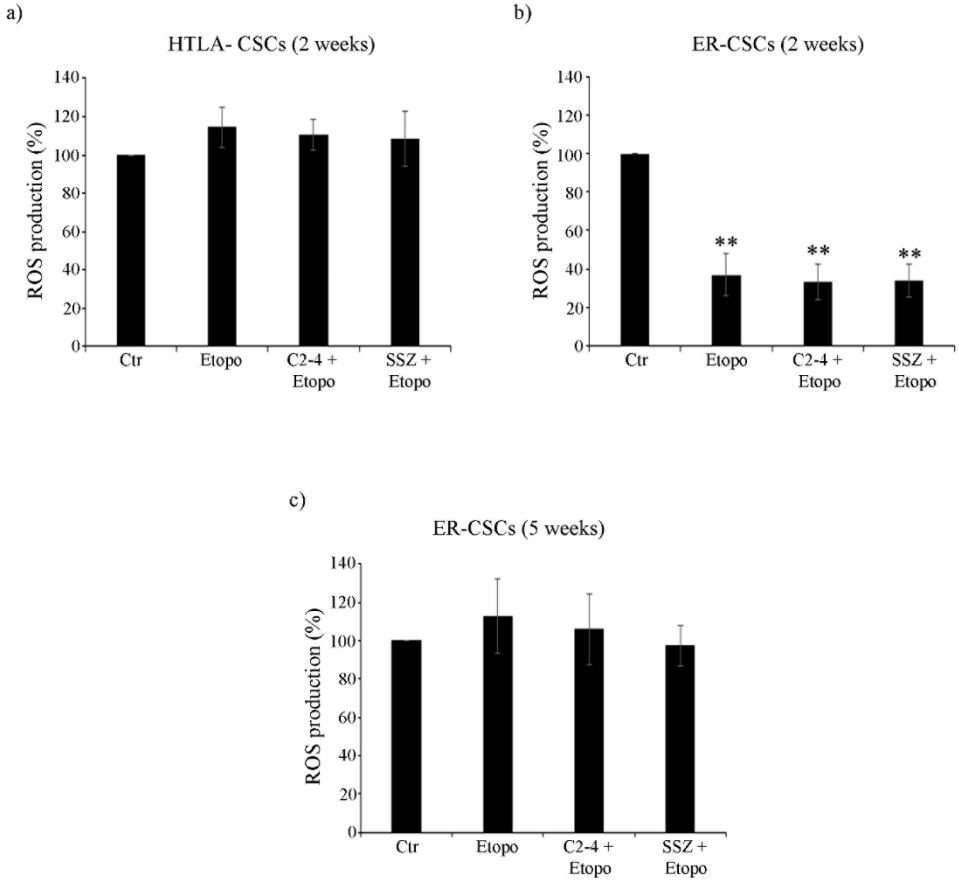

Figure 32. ROS production in both CSC populations treated for 2 (a, b) or 5 weeks (c). HTLA-CSCs and ER-CSCs were treated three times a week with 0.1 μM C2-4, with 5 μM SSZ or with 1.25 μM Etoposide, administered once a week alone or in combination with C2-4 or SSZ. Results were expressed as percentages of the control value. Bar graph summarizes quantitative data of means ± S.E.M. of three independent experiments. **$p<0.01$ vs. untreated CSCs (Ctr).

8.9. Co-treatments are able to induce down-regulation of GPX4 activity and of ZEB-1 expression

Taking into consideration that xCT inhibition has been demonstrated to induce lipid peroxide production and trigger ferroptosis, a form of non-apoptotic cell death consequent to GSH depletion and reduction of Glutathione peroxidase 4 (GPX4) activity (Yang W.S. et al., 2014; Maiorino M. et al., 2018), the role of this enzyme was investigated. As shown in Figure 33, after 5 weeks, in untreated ER-CSCs, GPX4 activity was reduced by 20% compared to that observed after 2 weeks. 2-week exposure to Etoposide, alone or in combination with SSZ, reduced the activity of GPX4 by 30% compared to that found in untreated CSCs. Instead, 2-week co-treatments with C2-4 further reduced GPX4 activity by 38% in comparison to Etoposide alone and by 55% in respect to the control. After 5 weeks, Etoposide, alone or in combination with C2-4, reduced GPX4 activity by 40% in respect to untreated CSCs, while SSZ co-treatments further inhibited the activity by 60% in comparison to Etoposide-treated CSCs and by 75% in respect to the control (Fig. 33).

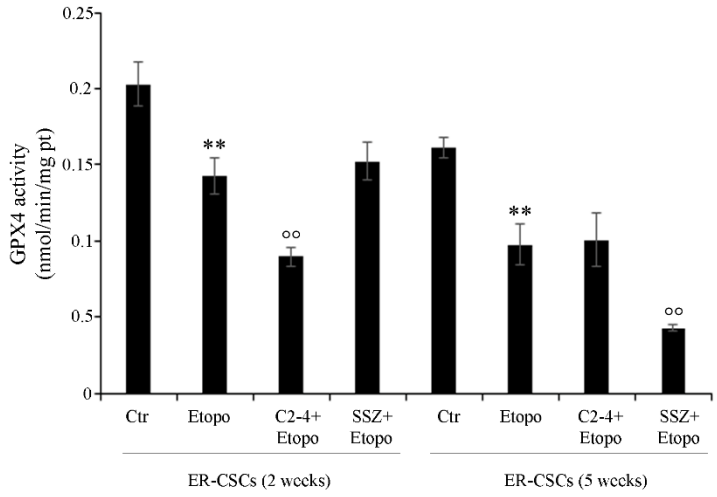

Figure 33. GPX4 activity in ER-CSC populations treated for 2 or 5 weeks. ER-CSCs were treated three times a week with 0.1 μM C2-4, with 5 μM SSZ or with 1.25 μM Etoposide, administered once a week alone or in combination with C2-4 or SSZ. Results were reported as nmol/min/mg protein. Bar graph summarizes quantitative data of means ± S.E.M. of three independent experiments. **p<0.01 vs. untreated ER-CSCs (Ctr); °°p<0.01 vs. Etoposide-treated ER-CSCs.

In this context, it has been reported that chemoresistant cancer cells, that are protected from ferroptosis through GPX4 activation, expressed high levels of ZEB-1, which is a protein involved in EMT process and playing a crucial role in supporting CSC generation (Viswanathan V.S. et al., 2017; Celia-Terrassa T. et al., 2020; Caramel J. et al., 2018). Based on these considerations, the subsequent analyses were focused on investigating the role played by EMT in chemoresistance. As shown in Figure 34a, both untreated CSC populations expressed N-Cadherin and ZEB-1, two proteins favoring the EMT process. In HTLA-CSCs, all 2 week-treatments totally abolished the expression of these two proteins while, interestingly, in ER-CSCs, only 2 week-Etoposide treatment was able to reduce the expression of N-Cadherin and ZEB-1 by 40% and 70%

respectively, in comparison to untreated CSCs (Fig. 34a and b). After 5 weeks the combination of Etoposide with C2-4 reduced the expression of both proteins by 50% and co-treatment with SSZ decreased ZEB-1 levels by 90% in respect to untreated CSCs (Fig. 34a and b). As shown in Figure 34c, changes in the expression of N-cadherin and ZEB-1 were not accompained by significant alterations in the expression of Vimentin and β-catenin, another two EMT-related proteins. Furthermore, Claudin, a protein able to inhibit EMT, was expressed only in treated HTLA-CSCs (Fig. 34d).

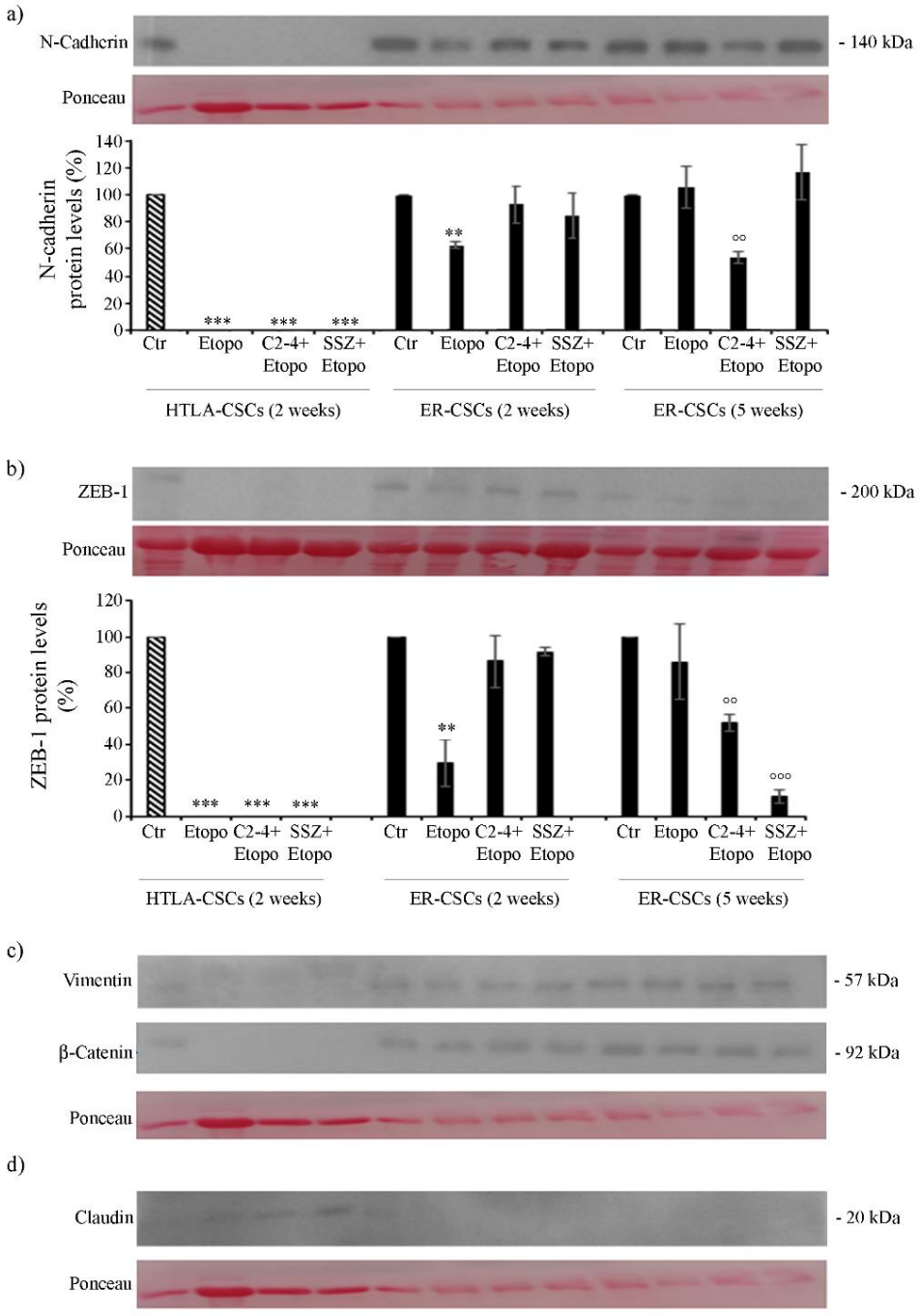

Figure 34. Protein levels of N-Cadherin (a), ZEB-1 (b), Vimentin (c), β-Catenin (c) and Claudin (d) in both CSC populations treated for 2 or 5 weeks. HTLA-CSCs and ER-CSCs were treated three times a week with 0.1 μM C2-4, with 5 μM SSZ or with 1.25 μM Etoposide, administered once a week alone or in combination with C2-4 or SSZ. Immunoblots shown are representative of three independent experiments. To ensure normalized protein content all filters were stained with Red Ponceau. Bar graph summarizes quantitative data of means ± S.E.M. of three independent experiments. **p<0.01 vs. untreated CSCs (Ctr); ***p<0.001 vs. untreated CSCs (Ctr); °°p<0.01 vs. Etoposide-treated CSCs; °°° p<0.001 vs. Etoposide-

treated CSCs. The original not-cropped images are reported as supplementary material at page 94.

8.10. Chemoresistance of ER-CSCs is characterized by an efficient OXPHOS metabolism, high GSH levels, ZEB-1 up-regulation and GPX4 activation.

In order to identify which variables are more determinant in maintaining cancer stem cell survival and, consequently, responsible for chemoresistance, Principal Component Analysis (PCA) was carried out by collecting all the analyzed metabolic, biochemical and morphological variables. The first two components explain 45.2% and 19.5% of the variance (64.6% in total).

The loading plot reported in Figure 35a shows the correlation between the following variables: P/O ratio, ATP production, GSH levels, ZEB-1 expression and GPX4 activity which are all characterized by negative loadings on PC1 (grouped in the green rectangle) and are all related since they allow the propagation of ER-CSCs. On the other side of the plot (positive loadings on PC1) another group of correlated variables can be detected (red rectangle): lactate release, glucose consumption and MDA production which reduce ER-CSC propagation and are responsible for their susceptibility to the co-treatments. The two groups of correlated variables are negatively correlated, since they are opposite compared to the origin (red cross in the plot). Furthermore, it is possible to identify a third group of correlated variables including by N-cad, OCR and Vim, which, by having high loadings on PC2, are uncorrelated with the other ones.

As expected from loading plot, the score plot (Figure 35b) shows that the 2-week and 5-week controls are close to each other, by having negative PC1 scores. Therefore, they are characterized by the high values of the variables

grouped into the green rectangle and the low values of the variables grouped into the red rectangle in the loading plot.

The effect of the three different treatments and of the different times, together with the metabolic modifications involved, can be estimated by taking into account the distance and the direction of the different points in the score plot, compared to the controls.

First of all, in the score plot shown in Fig. 35b, it can be seen that for both cell populations the effect after 5 weeks is larger than that observed after 2 weeks. Furthermore, the treatment with Etoposide by itself is much less efficient than the other treatments in which the chemotherapeutic drug is associated with SSZ or C2-4. In fact, although these co-treatments have almost no effect after 2 weeks, after 5 weeks they lead to a more positive score on PC1, indicating a reduction of the "green" variables and an increase of the "red" ones. By comparing the effect of SSZ or C2-4 on the action of Etoposide, it has been found that the co-treatment with SSZ has a much greater effect, already relevant after 2 weeks (corresponding to the effect after 5 weeks of Etoposide by itself). Since the direction is the same as the one already observed with Etoposide, it can be concluded that SSZ just amplifies the effect of Etoposide.

Instead, the co-treatment with C2-4 has a strong effect already at 2 weeks, but the trajectory followed is quite different from that of the Etoposide: an increase along PC1 together with a decrease along PC2 is observed, corresponding to a decrease of N-Cad, OCR and Vim variables. For these reasons, it can therefore be concluded that C2-4 not only amplifies the effect of Etoposide as observed for SSZ, but also produces different metabolic variations.

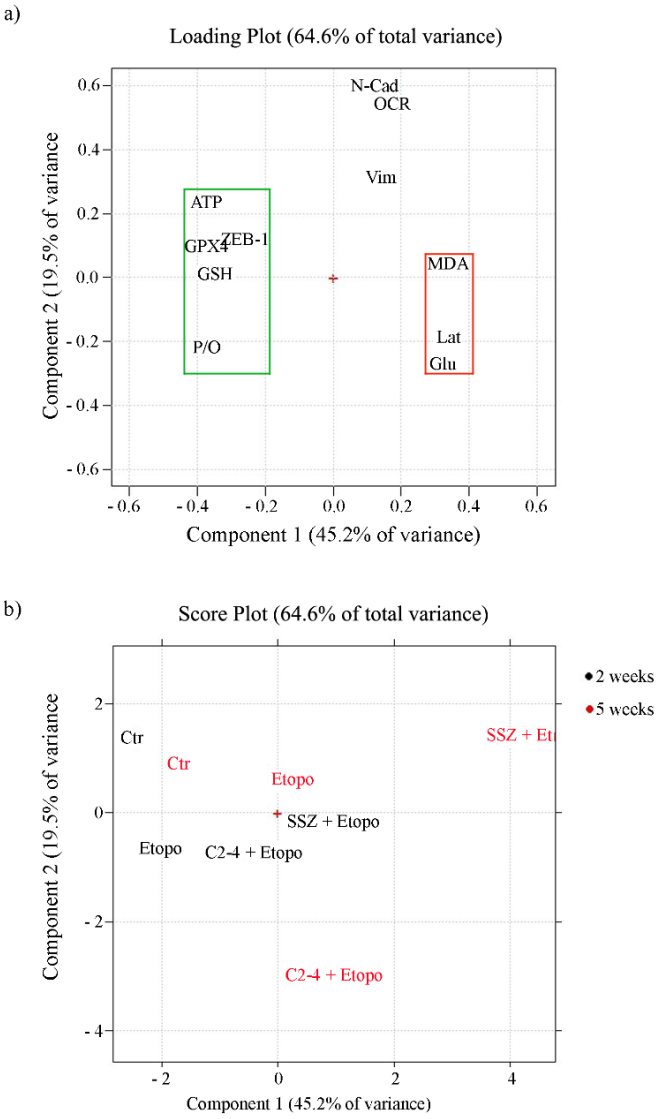

Figure 35. Loading (a) and score (b) plots of metabolic, biochemical and morphological variables. (a) The variables which sustain chemoresistance (green rectangle: ATP, GSH, P/O, ZEB-1, GPX4) have negative loadings on PC1 values, while the variables that are able to induce chemosensitivity (red rectangle: MDA production, lactate release and glucose consumption) have positive loadings on PC1; variables N-CAD, OCR and Vim have instead high loadings on PC2 (b) In the score plot, the black-colored samples were treated for 2 weeks, while the red-colored ones were treated for 5 weeks.

9. Discussion

Aging is associated with loss of cell homeostasis, deregulation of signaling pathways, genomic/epigenetic alterations and reduction of DNA repair that may lead to the development of aberrant cells giving rise to tumors. Therefore, aging is a determining factor in the development of cancer whose incidence increases with age (Schumacher B. et al., 2021). Moreover, it has been reported that aged patients have a poor response to anticancer therapy.

Despite the progress in the research finalized to produce effective anticancer drugs, several problems related to their toxic effects and the acquisition of therapy resistance remain still unsolved.

Chemoresistance can be of two types: i) intrinsic, which is an innate property of neoplastic cells that escape the effects of chemotherapy and ii) extrinsic, which is acquired by some cells following genetic and epigenetic mutations that arise during pharmacological treatments (Wang S. et al., 2019; Michelle X. et al., 2012). Chemoresistance is the result of many factors such as reduced drug intake and/or enhanced drug inactivation, changes in DNA damage response and apoptosis pathways, rewiring of oxidative metabolism, increased rate of cancer stem cells and EMT stimulation (Housman G. et al., 2014).

In this regard, our previous studies showed that GSH, the most important intracellular antioxidant thiol, plays a crucial role in mediating chemoresistance in human neuroblastoma cells resistant to Etoposide (Colla R. et al., 2016; Traverso N. et al., 2013) whose cytotoxic action is ROS-mediated (Sordet O. et al., 2004). Herein, the results reported demonstrate that GSH is implicated in the formation and maintenance of CSCs and suggest that the thiol depletion could be employed to increase sensitivity of CSCs to therapeutic approaches.

However, although BSO, a GSH-depleting agent, has been found to counteract CSC formation (Miran T. et al., 2018; Boivin A. et al., 2011; Siemann D.W. et al., 2011) and has been included in clinical trials (Villablanca J.G. et al., 2016), its therapeutic use is limited by its short half-life and by its non-selective depleting effects (Hamilton D. et al., 2007). Therefore, finding new strategies to deplete GSH content in cancer cells limiting the systemic side-effects is crucial. Looking at possible GSH-related targets, a particular attention has been given to CD44, a known stemness membrane marker (Nagano O. et al., 2004; Okamoto I. et al., 1999), and, in particular, to its variant 9 (CD44v9) that has been found to stabilize xCT, an anti-port protein involved in the cystine uptake and consequently in GSH biosynthesis.

Therefore, potential strategies to down-regulate GSH levels of CSCs could be to target xCT or CD44. Specifically, SSZ, an inhibitor of xCT, has been reported to be a good approach to deplete GSH (Zheng Z. et al., 2020; Wei C.W. et al., 2019; Ogihara K. et al., 2019; Miyoshi S. et al., 2018; Wada F. et al., 2018; Balza E. et al., 2017) but its use in clinic is limited due to its low bioavailability.

In addition, given that it has been demonstrated that the expression of CD44 is modulated by protein kinase C (PKC)-α (Nagano O. et al., 2004; Okamoto I. et al., 1999), the use of a PKC inhibitor could reduce CD44 expression and, consequently, limit the intracellular GSH availability.

Herein, the co-treatments with SSZ or with C2-4, a PKC-α inhibitor, are able to sensitise ER-CSCs to Etoposide by counteracting neurosphere formation. With regard to the strategy of PKC inhibition, a large number of studies have reported the efficacy of PKC-α inhibitors in sensitizing cancer cells to chemotherapeutic drugs (Lei J. et al., 2016; Kim C.W. et al., 2016; Abera M.B. et al., 2015; Ruvolo P.P. et al., 2011) and several clinical trials (NCT00042679; NCT00003236;

NCT00017407) have been carried out by using Aprinocarsen, an anti-sense oligonucleotide that targets PKC alpha mRNA, even if, unfortunately, the results obtained are not encouraging (Mochly-Rosen D. et al., 2012).

However, the analysis of GSH under all conditions of treatment confirms that the tripeptide is essential to support CSC survival but on other hand suggests that other factors might be involved since Etoposide, even though exerting a severe GSH-depleting action, does not totally counteract CSC generation.

In this regard, by taking into consideration that chemoresistant cancer cells (Colla R. et al., 2016; Vazquez F. et al., 2013; Viale A. et al., 2014) have been demonstrated to activate OXPHOS with a major ATP production as a therapy-adaptation strategy (Shin M.K. et al., 2019; Lagadinou E.D. et al., 2013; Molina J.R. et al., 2018; Pollyea D.A. et al., 2018), the role of metabolism has been investigated.

As reported in previous studies (Sato M. et al., 2016; Denise C. et al., 2015) demonstrating that this metabolic rewiring can be reversible, in our model the co-treated ER-CSCs return to activate glycolysis as Etoposide-sensitive cancer cells. Moreover, according to previous studies (Yang W.S. et al., 2014; Maiorino M. et al., 2018; Su Y. et al., 2020), herein we demonstrate that SSZ co-treatment induces GSH depletion, GPX4 inactivation and lipid peroxidation triggering ferroptosis, a form of non-apoptotic cell death. Notably, we report for the first time that also C2-4-co-treatment is able to sensitize ER-CSC to Etoposide *via* depletion of GSH levels and reduction of GPX4 activity.

C2-4, analogously to SSZ, acts as GPX4 inhibitor and could be used to counteract the onset of chemoresistance through induction of ferroptosis (Seibt T.M. et al., 2019). In this context, it has been reported that chemoresistant cancer cells, that are preserved from ferroptosis *via* GPX4 activation, display high levels

of ZEB-1 (Viswanathan V.S. et al., 2017). ZEB-1 is a central driver of EMT process and, as described in the introduction, plays an important role in CSC generation (Brabletz T. et al., 2005; Brabletz S. et al., 2010; Brabletz T., 2012; Celia-Terrassa T. et al., 2020). In fact, ZEB-1 has been found to have a pleiotropic role in controlling lipid metabolism, growth, proliferation and death of CSCs (Viswanathan V.S. et al., 2017; Caramel J. et al., 2018).

Herein, we report that the co-treatments with SSZ or C2-4 counteract the ability of ER-CSCs to generate spheres and to maintain the mesenchymal phenotype, by down-regulating ZEB-1 expression and leading to ferroptosis. This *in vitro* data is in line with the results observed in early clinical trials demonstrating that the disruption of cancer stemness and/or the EMT process is a useful approach in fighting tumor recurrence (Rodriguez-Aznar E. et al., 2019; Shibue T. et al., 2017).

While our results have confirmed the ferroptotic-inducer action of SSZ, this is the first time, to our knowledge, that an anti-PKC peptide has been shown to sensitize CSCs to chemotherapy by inhibiting GPX4 and inducing ferroptosis. However, the ferroptotic action of C2-4 co-treatment could be definitely confirmed in the next future by using a specific ferroptosis inhibitor such as Ferrostatin-1 (Miotto G. et al., 2020).

In support of this hypothesis, it has been demonstrated that the pharmacologic inhibition of PKC-α can target breast CSCs (Tam W.L. et al., 2013) and override ZEB1-induced chemoresistance in hepatocarcinoma (Sreekumar, R. et al., 2019).

Finally, PCA analysis carried out by collecting all the analyzed metabolic, biochemical and morphological variables underline that chemoresistance of ER-CSCs is characterized by an efficient OXPHOS metabolism, high GSH levels, ZEB-1 up-regulation and GPX4 activation that lead to a complex cellular

adaptation responsible for cancer survival and recurrence. Therefore, it is necessary to focus the attention and to monitor these variables in order “to attack the enemy” simultaneously from several fronts and bypass these strategies of adaptation.

However, even if the mechanisms underlying CSC chemoresistance need to be further clarified, the results of this thesis suggest that drug refractoriness is maintained as long as CSCs are able to keep a fine balance between some correlated molecular actors: the activation of an oxidative metabolism, the maintenance of high levels of GSH and of ZEB-1 expression that concur to guarantee the survival of resistant CSCs. Therefore, an approach able to down-regulate these molecular targets and to induce ferroptosis may be the winning strategy to counteract drug resistance. Notably, the results herein reported suggest that PKC-α might be a new pharmacological target able to fight chemoresistance of CSCs by preventing drug-induced metabolic adaptation and triggering ferroptotic death.

Starting from these encouraging results, additional experiments of PKC-α modulation (silencing/overexpression) and *in vivo* treatments with C2-4 will be necessary in order to confirm the efficacy of PKC-α inhibition in the sensitization of cancer stem cells to the therapy.

10. Bibliography

Abera M.B., Kazanietz M.G. - Protein kinase Cα mediates erlotinib resistance in lung cancer cells. Mol. Pharmacol. 87, 832–841; 2015.

Aguilar-Gallardo C., Simon C. - Cells, stem cells, and cancer stem cells. Semin Reprod Med. 31(1):5–13; 2013.

Aguirre-Ghiso J.A. - Models, mechanisms and clinical evidence for cancer dormancy. Nat Rev Cancer. 7:834–46; 2007.

Aigner K., Dampier B. etal. - The transcription factor ZEB1 (deltaEF1) promotes tumour cell dedifferentiation by repressing master regulators of epithelial polarity. Oncogene, 25;26(49):6979-88; 2007.

Ali Osman F. et al. - Decreased DNA Interstrand Cross-Linking and Cytotoxicity Induced in Human Brain Tumor Cells by 1,3-Bis(2-chloroethyl)-1-nitrosourea after in Vitro Reaction with Glutathione. Cancer Research 49, Issue 21; 1989.

Anjomshoaa A., Nasri S., Humar B., Mccall J.L., Chatterjee A., Yoon H.S. et al. - Slow proliferation as a biological feature of colorectal cancer metastasis. Br J Cancer. 101:822–8; 2009.

Asensi M., Sastre J. et al. - Ratio of reduced to oxidized glutathione as indicator of oxidative stress status and DNA damage. Methods Enzymol. 299, 267–276; 1999.

Babu K.R., Muckenthaler M.U. - miR-20a regulates expression of the iron exporter ferroportin in lung cancer. J Mol Med (Berl). 94:347–59; 2016.

Backos S. et al. - The role of glutathione in brain tumor drug resistance. Biochemical Pharmacology Volume 83, Issue 8, 1005-1012; 2012.

Balkwill F., Mantovani A. - Inflammation and cancer: Back to Virchow? Lancet; 2001.

Bates A.D., Maxwell A. - DNA topology: topoisomerases keep it simple. Curr Biol 7: 778-81; 1997.

Berger N.A., Savvides P. et al. - Cancer in the Elderly Trans. Am. Clin. Clim. Assoc., 117, 147-156; 2006.

Bharti R., Dey G., Mandal M. - Cancer development, chemoresistance, epithelial to mesenchymal transition and stem cells: a snapshot of IL-6 mediated involvement. Cancer Lett.; 2016.

Boivin A., Hanot M. et al. - Transient alteration of cellular redox buffering before irradiation triggers apoptosis in head and neck carcinoma stem and non-stem cells. PLoS ONE, 6, e14558; 2011.

Bolos V., Peinado H., Perez-Moreno M.A., Fraga M.F., Esteller M., Cano A. - The transcription factor Slug represses E-cadherin expression and induces epithelial to mesenchymal transitions: a comparison with Snail and E47 repressors. Journal of Cell Science 116(Pt 3):499-511; 2003.

Bonnans C., Chou J., Werb Z. - Remodelling the extracellular matrix in development and disease. Nat. Rev. Mol. Cell Biol. 15, 786-801; 2014.

Brabletz T. - EMT and MET in Metastasis: Where Are the Cancer Stem Cells? Cancer Cell 22; 2012.

Brabletz S., Brabletz T. - The ZEB/miR-200 feedback loop--a motor of cellular plasticity in development and cancer? EMBO Rep. 11, 670-677; 2010.

Brabletz T., Jung A., Spaderna S., Hlubek F., Kirchner T. - Opinion: migrating cancer stem cells - an integrated concept of malignant tumour progression. Nat Rev Cancer. 5, 744-749, 2005.

Brigelius- Flohe R., Maiorino M. - Glutathione peroxidases. Biochim. Biophys. Acta 1830, 3289-3303; 2013.

Brigelius-Flohe R. - Tissue specific functions of individual glutathione peroxidases. Free Radic. Biol. Med. 27: 951-965;1999.

Brown N.H. - Extracellular matrix in development: Insights from mechanisms conserved between invertebrates and vertebrates. Cold Spring Harb. Perspect Biol. 3, 1–13; 2011.

Cano A., Perez-Moreno M.A., Rodrigo I., Locascio A., Blanco M.J., del Barrio M.G. etal. - The transcription factor snail controls epithelial-mesenchymal transitions by repressing E-cadherin expression. Nature Cell Biology 2(2):76-83; 2000.

Caramel J., Ligier M., Puisieux A. - Pleiotropic Roles for ZEB1 in Cancer. Cancer research 78 (1); 2018.

Castriconi R. et al. - Human NK cell infusions prolong survival of metastatic human neuroblastoma-bearing NOD/scid mice. Cancer Immunol Immunother 56:1733–1742; 2007.

Celià-Terrassa T., Jolly M.K. -Cancer Stem Cells and Epithelial-to-Mesenchymal Transition in Cancer Metastasis. Cold Spring Harb. Perspect. Med.; 2020.

Chen F., Zhuang X. et al. - New horizons in tumor microenvironment biology: Challenges and opportunities. BMC Med. 13; 2015.

Cheong J.H., Park E.S. et al. - Dual inhibition of tumor energy pathway by 2-deoxyglucose and metformin is effective against a broad spectrum of preclinical cancer models. Mol Cancer Ther. 10(12):2350–62; 2011.

Chung J.H., Rho J.K. et al. - Clinical and molecular evidences of epithelial to mesenchymal transition in acquired resistance to EGFRTKIs. Lung Cancer; 2010.

Colla R., Izzotti A., De Ciucis C. et al. - Glutathione-mediated antioxidant response and aerobic metabolism: two crucial factors involved in determining the multi-drug resistance of high-risk neuroblastoma. Oncotarget. 25; 7: 70715-70737; 2016.

Cozza G., Rossetto M. et al. - Glutathione peroxidase 4-catalyzed reduction of lipid hydroperoxides in membranes: The polar head of membrane phospholipids binds the enzyme and addresses the fatty acid hydroperoxide group toward the redox center. Free Radical Biology and Medicine Volume 112, 1-11; 2017.

De Francesco E.M., Sotgia F., Lisanti M.P. - Cancer stem cells (CSCs): metabolic strategies for their identification and eradication - Biochem J.; 2018.

De Luca A., Fiorillo M., Peiris-Pages M., Ozsvari B., Smith D.L., Sanchez-Alvarez R. etal. - Mitochondrial biogenesis is required for the anchorageindependent survival and propagation of stem-like cancer cells. Oncotarget. 6(17):14777–95; 2015.

Dempsey E.C., Newton A.C., Mochly-Rosen D. et al. - Protein kinase C isozymes and the regulation of diverse cell responses. Am J Physiol 279: L429–38; 2000.

Denise C., Paoli P., Calvani M. et al. - 5-fluorouracil resistant colon cancer cells are addicted to OXPHOS to survive and enhance stem-like traits. Oncotarget 6, 41706–41721; 2015.

Diehn M., Cho R.W., Lobo N.A., Kalisky T., Dorie M.J., Kulp A.N. et al. - Association of reactive oxygen species levels and radioresistance in cancer stem cells. Nature. 458(7239):780–3; 2009.

Dixon S. J. et al. - Human haploid cell genetics reveals roles for lipid metabolism genes in nonapoptotic cell death. ACS Chem. Biol. 10, 1604–1609; 2015.

Dixon S.J., Lemberg K.M., Lamprecht M.R. et al. - Ferroptosis: an iron-dependent form of nonapoptotic cell death. Cell 149:1060–1072; 2012.

Dixon S.J., Stockwell B.R. - The role of iron and reactive oxygen species in cell death. Nat. Chem. Biol. 10, 9–17; 2014.

Doktorova H., Hrabeta J., Mohamed Ashraf Khalil M., Eckschlager T. - Hypoxia-induced chemoresistance in cancer cells: The role of not only HIF-1. Biomed Pap Med Fac Univ Palacky Olomouc Czech Repub. 159(2):166-177; 2015.

Doll S. et al. - ACSL4 dictates ferroptosis sensitivity by shaping cellular lipid composition. Nat. Chem. Biol. 13, 91–98; 2017.

Doll S., Porto Freitas F. et al. - FSP1 is a glutathione-independent ferroptosis suppressor. Nature doi:10.1038/s41586-019-1707-0; 2019.

Dupuy F., Tabaries S., Andrzejewski S., Dong Z., Blagih J., Annis M.G. et al. - PDK1-dependent metabolic reprogramming dictates metastatic potential in breast cancer. Cell Metab. 22(4):577–89; 2015.

Eger A., Aigner K., Sonderegger S., Dampier B. et al. – Delta EF1 is a transcriptional repressor of E-cadherin and regulates epithelial plasticity in breast cancer cells. Oncogene 24:2375-85; 2005.

Evans C.G. et al. - Glutathione and Related Enzymes in Rat Brain Tumor Cell Resistance to 1,3-Bis(2-chloroethyl)-1-nitrosourea and Nitrogen Mustard. Cancer Research 47, Issue 10; 1987.

Farber S., Diamond L. K. - Temporary remissions in acute leukemia in children produced by folic acid antagonist, 4-aminopteroyl-glutamic acid. N. Engl. J. Med. 238, 787–793; 1948.

Fariss M.W., Reed D.J. - High-performance liquid chromatography of thiols and disulfides: Dinitrophenol derivatives. Methods Enzymol.143, 101–109; 1987.

Farnie G., Sotgia F., Lisanti M.P. - High mitochondrial mass identifies a subpopulation of stem-like cancer cells that are chemo-resistant. Oncotarget. 6(31):30472–86; 2015.

Finkel T., Serrano M., Blasco M.A. - The common biology of cancer and ageing. Nat. Cell Biol., 448, 767–774; 2007.

Folkman J. - Role of angiogenesis in tumor growth and metastasis. Semin Oncol. 29:15–8; 2002.

Ford J., Hait W. - Pharmacology of drugs that alter multidrug resistance in cancer. Pharmacol Rev 42: 156–99; 1990.

Frantz C., Stewart K.M., Weaver V.M. - The extracellular matrix at a glance. J. Cell Sci. 123, 4195 4200; 2010.

Friedmann Angeli J.P., Krysko V., Conrad M. - Ferroptosis at the crossroads of cancer- acquired drug resistance and immune evasion. Nature reviews; 2019 (a).

Friedmann Angeli J. P., Miyamoto S., Schulze A. - Ferroptosis: the greasy side of cell death. Chem. Res. Toxicol. 32, 362–369; 2019 (b).

Friedmann Angeli J.P. et al. - Inactivation of the ferroptosis regulator Gpx4 triggers acute renal failure in mice. Nat. Cell Biol. 16, 1180–1191; 2014.

Friedmann Angeli J.P., Conrad, M. - Selenium and GPX4, a vital symbiosis - Free Radic. Biol. Med. 127, 153–159; 2018.

Fukai, T., Ushio-Fukai M. - Superoxide Dismutases: Role in Redox Signaling, Vascular Function, and Diseases. Antioxid. Redox Signal. 15: 1583-1606; 2011.

Galluzzi L et al. - Molecular mechanisms of cisplatin resistance. Oncogene. 12;31(15):1869-83; 2012.

Gammon L., Biddle A., Hannah A. et al. - Sub-Sets of Cancer Stem Cells Differ Intrinsically in Their Patterns of Oxygen Metabolism. PLoS ONE 8(4): e62493. 2013.

Gao M., Monian P., Jiang X. - Metabolism and iron signaling in ferroptotic cell death. Oncotarget 6(34):35145-6; 2015.

Gattazzo F., Urciuolo A., Bonaldo P. - Extracellular matrix: A dynamic microenvironment for stem cell niche. Biochim. Biophys. Acta 1840, 2506–2519; 2014.

Gatto B., Leo E. - Drugs acting on the beta isoform of human topoisomerase II. Curr Med Chem 3:175–85; 2003.

Gilman A. - The initial clinical trial of nitrogen mustard. Am J Surgery 105: 574–8; 1963.

Guppy M., Greiner E., Brand K. - The role of the Crabtree effect and an endogenous fuel in the energy metabolism of resting and proliferating thymocytes. Eur J Biochem. 212(1):95–9; 1993.

Halliwell B., Gutteridge J.M.C. - Free Radicals in Biology and Medicine, 5th ed.; Oxford University Press: Oxford, NY, USA; ISBN 978-0-19-871748-5; 2015.

Hamed A.R., Abdel N.S., Shams K.A. et al. - Targeting multidrug resistance in cancer by natural chemosensitizers. Bull Natl Res Cent 43:8; 2019.

Hamilton D., Wu J.H., Batist G. - Structure-based identification of novel human gamma-glutamylcysteine synthetase inhibitors. Mol. Pharmacol., 71, 1140-1147; 2007.

Hanahan D., Coussens L.M. - Accessories to the crime: Functions of cells recruited to the tumor microenvironment. Cancer Cell 21, 309–322; 2012.

Hanahan D., Folkman J. - Patterns and emerging mechanisms of the angiogenic switch during tumorigenesis. Cell. 86 353–364; 1996.

Helleday T. - Homologous recombination in cancer development, treatment and development of drug resistance. Carcinogenesis, Volume 31, Issue 6, 955–960; 2010.

Hinkle P.C. - P/O ratios of mitochondrial oxidative phosphorylation. Biochim. Biophys. Acta, 1706, 1–11; 2005.

Ilkhani F., Hosseini B., Saedisomeolia A. - Niacin and oxidative stress: a Mini-review. J. Nutri. Med. Diet Care 2; 2016.

Housman G., Byler S., Heerboth S., Lapinska K., Longacre M., Snyder N., Sarkar S. - Drug resistance in cancer: an overview. Cancers (Basel), 5;6(3):1769-92; 2014.

Ingold I., Roveri A. et al. - Selenium utilization by GPX4 is required to prevent hydroperoxide-induced ferroptosis. Cell 172, 409–422.e21; 2018.

Ishimoto T., Nagano O., Yae T. et al. - CD44 variant regulates redox status in cancer cells by stabilizing the xCT subunit of system xc(-) and thereby promotes tumor growth. Cancer Cell, 19, 387–400; 2011.

Ji X., Qian J., Rahman S.M.J., Siska P.J. et al. - xCT (SLC7A11)-mediated metabolic reprogramming promotes non-small cell lung cancer progression. Oncogene. 37: 5007-5019; 2018.

Jung Y. D., Ahmad S.A. et al. - Role of the tumor microenvironment in mediating response to anti-angiogenic therapy. Cancer Metastasis Rev.; 2000.

Kawano Y., Okamoto I., Murakami D., Itoh H., Yoshida M., Ueda S., Saya H. - Ras oncoprotein induces CD44 cleavage through phosphoinositide 3-OH kinase and the rho family of small G proteins. J Biol Chem 275: 29628– 35; 2000.

Kawano T., Inokuchi J., Eto M., Murata M., Kang J.H. - Activators and Inhibitors of Protein Kinase C (PKC): Their Applications in Clinical Trials. Pharmaceutics. 20;13(11):1748; 2021.

Kellner U., Sehested M., Jensen P.B., Gieseler F., Rudolph P. - Culprit and victim-DNA topoisomerase II. Lancet Oncol 3:235–43; 2002.

Kim C.W., Asai D., Kang J., Kishimura A., Mori T., Katayama Y. - Reversal of efflux of an anticancer drug in human drugresistant breast cancer cells by inhibition of protein kinase Cα (PKCα) activity. Tumour. Biol. 37, 1901-1908; 2016.

Koppenol W.H., Bounds P.L., Dang C.V. - Otto Warburg's contributions to current concepts of cancer metabolism. Nat. Rev. Cancer 11, 325–337; 2011.

Kushner B.H., Helson L., Lane J.M., Hajdu S.I. - Metastatic neuroblastoma after 52 years of apparent dormancy. N Engl J Med. 315:196–7; 1986.

Lagadec C., Meignan S., Adriaenssens E., Foveau B., Vanhecke E., Romon R. et al. - TrkA overexpression enhances growth and metastasis of breast cancer cells. Oncogene 28(18):1960–70; 2009.

Lagadinou E.D., Sach A. et al. - BCL-2 inhibition targets oxidative phosphorylation and selectively eradicates quiescent human leukemia stem cells. Cell Stem Cell, 12, 329–341; 2013.

Lamouille S. et al. - Molecular mechanisms of epithelial–mesenchymal transition Nat Rev Mol Cell Biol. 15(3): 178–196; 2014.

Larsson R., Nygren P. - Laboratory prediction of clinical chemotherapeutic drug resistance: a working model exemplified by acute leukaemia. Eur J Cancer 29A: 1208–12; 1993.

Leardi R. - Chemometric methods in food authentication". Modern techniques for food authentication (Second Edition). Elsevier, 687-729; 2018.

Leardi R., Melzi C., Polotti G. - CAT (Chemometric Agile Software). Available online: http://gruppochemiometria.it/index.php/Software

Lei J., Li Q. et al. - Increased PKCα activity by Rack1 overexpression is responsible for chemotherapy resistance in T-cell acute lymphoblastic leukemia-derived cell line. Sci. Rep., 6, 33717; 2016.

Liang D., Deng L., Jiang X. - A new checkpoint against ferroptosis. Cell Res. 30(1):3-4; 2020.

Liao J., Qian F., Tchabo N., Mhawech-Fauceglia P. et al. - Ovarian cancer spheroid cells with stem cell-like properties contribute to tumor generation, metastasis and chemotherapy resistance through hypoxia-resistant metabolism. PLoS One. 9(1); 2014.

Liu J., Xiaojun X., Peng H. - xCT: A Critical Molecule That Links Cancer Metabolism to Redox Signaling. Molecular Therapy, Vol. 28, 2358-2366; 2020.

Liu S., Ye D. et al. - G9a is essential for EMT-mediated metastasis and maintenance of cancer stem cell-like characters in head and neck squamous cell carcinoma. Oncotarget. 6(9): 6887–6901; 2015.

Lo M. et al. - The xC^- Cystine/Glutamate Antiporter: A Potential Target for Therapy of Cancer and Other Diseases. and/or sensitizing cancers is discussed. J. Cell. Physiol. 215: 593–602, 2008.

Lu H., Sanjun S. Gong T. et al. - Cancer stem cells: therapeutic implications and perspectives in cancer therapy. Acta Pharmaceutica Sinica B Volume 3, Issue 2 , 65-75; 2013.

Ma M.Z., Chen G., Wang P., et al. - Xc- inhibitor sulfasalazine sensitizes colorectal cancer to cisplatin by a GSH-dependent mechanism. Cancer Lett. 1; 368: 88-96; 2015.

Maiorino M., Conrad M., Ursini F. - GPx4, lipid peroxidation, and cell death: discoveries, rediscoveries, and open issues. Antioxid Redox Signal.29(1):61-74; 2018.

Malik R., Lelkes P.I., Cukierman E. - Biomechanical and biochemical remodeling of stromal extracellular matrix in cancer. Trends in biotechnology, 2015.

Mani S.A., Guo W., Liao M.J., Eaton E.N., Ayyanan A., Zhou A.Y. et al. - The epithelial–mesenchymal transition generates cells with properties of stem cells. Cell 133(4):704–15; 2008.

Mannervik B. - Glutathione peroxidase - Methods Enzymol. 113:490-495; 1985.

Marengo B., Nitti M. et al. - C. Redox Homeostasis and Cellular Antioxidant Systems: Crucial Players in Cancer Growth and Therapy. Oxid Med Cell Longev. 6235641; 2016.

Martin H.L., Teismann P. - Glutathione–a review on its role and significance in Parkinson's disease. FASEB J. 23(10):3263-3272; 2009.

Masanori H., Hidekazu T., Hasan R., Maroof A., Yozo S., Li Y et al. - Functional interactions of the cystine/glutamate antiporter, CD44v and MUC1-C oncoprotein in triple-negative breast cancer cells. Oncotarget. 7:11756–69; 2016.

Massague J. - G1 cell-cycle control and cancer. Nature 432:298–306; 2004.

Matsushima H., Bogenmann E. - Modulation of neuroblastoma cell differentiation by the extracellular matrix. Int J Cancer. 51(5):727-32; 1992.

McHugh D., Gil J. - Senescence and aging: causes, consequences, and therapeutic avenues. J. Cell Biol., 217, 65–77; 2017.

Meister A. - Glutathione metabolism and its selective modification. J Biol Chem. 25;263(33):17205-8; 1988.

Miao L., St Clair D.K. - Regulation of Superoxide Dismutase Genes: Implications in Disease. Free Radic. Biol. Med. 47: 344-356; 2009.

Michael M., Doherty M.M. - Tumoral drug metabolism: Overview and its implications for cancer therapy. J. Clin. Oncol. 23, 205–229; 2005.

Michelle X., Liu David W., Chan Hextan Y.S. - Mechanisms of chemoresistance in human ovarian cancer at a glance. Gynecol. Obstet. 2 (3) PP1; 2012.

Miotto G., Rossetto M. et al. - Insight into the mechanism of ferroptosis inhibition by ferrostatin-1. Redox Biology; 2020.

Mir R., Phillips S.L., Schwartz G., Mathur R., Khan A., Kahn LB. - Metastatic neuroblastoma after 52 years of dormancy. Cancer 60:2510–4; 1987.

Miran T., Vogg A.T.J. et al. - Modulation of glutathione promotes apoptosis in triplenegative breast cancer cells. FASEB J, 32, 2803–2813; 2018.

Miyoshi S., Tsugawa H. et al. - Inhibiting xCT Improves 5-Fluorouracil Resistance of Gastric Cancer Induced by CD44 Variant 9 Expression. Anticancer Res., 38, 6163–6170; 2018.

Mochly-Rosen D., Das K., Grimes K.V. - Protein kinase C, an elusive therapeutic target? Nat. Rev. Drug Discov., 11, 937–957; 2012.

Molina J.R., Sun Y. et al. - An inhibitor of oxidative phosphorylation exploits cancer vulnerability. Nat. Med., 24, 1036–1046; 2018.

Monaco M.E. et al. - Expression of long-chain fatty acyl-CoA synthetase 4 in breast and prostate cancers is associated with sex steroid hormone receptor negativity. Transl. Oncol. 3, 91–98; 2010.

Moore N., Lyle S. - Quiescent, slow-cycling stem cell populations in cancer: a review of the evidence and discussion of significance. J Oncol.; 2011.

Morales M., García A.J. - Papel de la superfamilia ABC en la resistencia farmacológica. Horiz Sanit 16(2):93–101; 2017.

Morel A.P., Lievre M., Thomas C., Hinkal G., Ansieau S., Puisieux A. - Generation of breast cancer stem cells through epithelial–mesenchymal transition. PLoS One 3(8):e2888; 2008.

Mroue R., M.J. Bissell - Three-dimensional cultures of mouse mammary epithelial cells. Methods Mol. Biol.; 2013.

Müller L., Di Benedetto S., Pawelec G. - The Immune System and Its Dysregulation with Aging - In Biochemistry and Cell Biology of Ageing: Part II Clinical Science. Springer: Berlin/Heidelberg, Germany, 21–43; 2019.

Nagano O., Saya H. - Mechanism and biological significance of CD44 cleavage. Cancer Sci. 95, 930–935; 2004.

Nitiss J.L. - DNA topoisomerase II and its growing repertoire of biological functions. Nat Rev Cancer 9: 327-337; 2009.

Ogihara K., Kikuchi E. et al. - Sulfasalazine could modulate the CD44v9-xCT system and enhance cisplatin-induced cytotoxic effects in metastatic bladder cancer. Cancer Sci. 110, 1431–1441; 2019.

Okamoto I., Kawano Y., Matsumoto M., Suga M., Kaibuchi K., Ando M., Saya H. - Regulated CD44 cleavage under the control of protein kinase C, calcium influx, and the Rho family of small G proteins. J Biol Chem 274: 25525–34; 1999.

Okazaki F., Matsunaga N., Hamamura K., Suzuki K., Nakao T., Okazaki H., et al. - Administering xCT inhibitors based on circadian clock improves antitumor effects. Cancer Res. 77(23); 2017.

Oliveira S.S., Morgado-Díaz J.A. - Claudins: multifunctional players in epithelial tight junctions and their role in cancer. Cellular and Molecular Life Sciences volume 64, 17–28; 2007.

Orlando U.D. et al. - Acyl-CoA synthetase-4, a new regulator of mTOR and a potential therapeutic target for enhanced estrogen receptor function in receptor-positive and -negative breast cancer. Oncotarget 6, 42632–42650; 2015.

Papa S., Martino P.L. et al. - The oxidative phosphorylation system in mammalian mitochondria. Adv. Exp. Med. Biol. 942, 3–37; 2012.

Parri M., Chiarugi P. - Rac and Rho GTPases in cancer cell motility control. Cell Commun. Signal. 8, 23; 2010.

Patel H., Nilendu P. et al. - Modulating secreted components of tumor microenvironment: a masterstroke in tumor therapeutics. Cancer Biol. Ther. 19 3–12; 2018.

Pattabiraman D.R., Weinberg R.A. - Tackling the cancer stem cells—what challenges do they pose? Nat Rev Drug Discov. 13(7):497–512; 2014.

Peijing Z., Yutong S., Li M. - ZEB1: At the crossroads of epithelial-mesenchymal transition, metastasis cancer cells. Biochem J.;473(6):769-777; 2016.

Peiris-Pages M., Martinez-Outschoorn U.E., Pestell R.G., Sotgia F., Lisanti M.P. - Cancer stem cell metabolism. Breast Cancer Res.; 2016.

Perez-De Marcos J. C., Perez-Pineda P. L. et al. - ABC transporter superfamily. An updated overview, relevance in cancer multidrug resistance and perspectives with personalized medicine. Molecular Biology Reports, 48:1883–1901; 2021.

Pezzolo A. et al. - Tumor origin of endothelial cells in human neuroblastoma. J. Clin. Oncol. 25, 376–383; 2007.

Pogorelcnik B., Andrej Perdih A., Solmajer T. - Recent Developments of DNA Poisons - Human DNA Topoisomerase II Inhibitors as Anticancer Agents. Current Pharmaceutical Design 19, 2474-2488; 2013.

Pollyea D.A., Stevens B.M. et al. - Venetoclax with azacitidine disrupts energy metabolism and targets leukemia stem cells in patients with acute myeloid leukemia. Nat. Med., 24, 1859–1866; 2018.

Ponta H., Sherman L., Herrlich P.A. - CD44: from adhesion molecules to signalling regulators. Nat. Rev. Mol. Cell. Biol. 4: 33-45; 2003.

Powers S.K., Jackson M.J. - Exercise–induced oxidative stress: cellular mechanisms and impact on muscle force roduction. Physiol. Res. 88: 1243-1276; 2008.

Preca B.T., Bajdak K., Mock K., Brabletz S., Brabletz T. et al. - A self-enforcing CD44s/ZEB1 feedback loop maintains EMT and stemness properties in cancer cells. Int. J. Cancer: 137, 2566–2577; 2015.

Puisieux A., Brabletz T., Caramel J. - Oncogenic roles of EMT-inducing transcription factors. Nat Cell Biol 16:488–94; 2014.

Ravera S., Bartolucci M., Cuccarolo P. et al. - Oxidative stress in myelin sheath: The other face of the extramitochondrial oxidative phosphorylation ability. Free Radic Res. 49, 1156–1164; 2015.

Reya T., Morrison S.J., Clarke M.F., Weissman I.L. - Stem cells, cancer, and cancer stem cells. Nature, 414(6859):105-11; 2001.

Rodriguez-Aznar E., Wiesmüller L., Sainz B. Jr., Hermann P.C. - EMT and Stemness-Key Players in Pancreatic Cancer Stem Cells. Cancers 11, 1136; 2019.

Rohani M.G., Parks W.C. - Matrix remodeling by mmps during wound repair. Matrix Biol. 44–46, 113–121; 2015.

Roveri A., Maiorino M., Ursini F. - Enzymatic and immunological measurements of soluble and membrane-bound phospholipid-hydroperoxide glutathione peroxidase. Methods Enzymol. 233, 202–212; 1994.

Ruvolo P.P., Zhou L. et al. - Targeting PKC-mediated signal transduction pathways using enzastaurin to promote apoptosis in acute myeloid leukemia-derived cell lines and blast cells. J. Cell Biochem., 112, 1696–1707; 2011.

Sasaki H., Sato H., Kuriyama-Matsumura K. et al. Electrophile response element-mediated induction of the cystine/glutamate exchange transporter gene expression. J. Biol. Chem. 22; 277: 44765-71; 2002.

Sato M., Kawana K. et al. - Spheroid cancer stem cells display reprogrammed metabolism and obtain energy by actively running the tricarboxylic acid (TCA)cycle. Oncotarget, 7, 33297–33305; 2016.

Scheel C., Weinberg R.A. - Cancer stem cells and epithelial–mesenchymal transition: Concepts and molecular links. Seminars in Cancer Biology Volume 22, Issues 5–6, 396-403; 2012.

Schumacher B., Pothof J., Vijg J., Hoeijmakers Jan H.J. - The central role of DNA damage in the ageing process. Nature, Vol. 592; 2021.

Seibt T.M., Proneth B., Conrad M. - Role of GPX4 in ferroptosis and its pharmacological implication. Free Radic. Biol. Med. 133, 144–152; 2019.

Shen A., Zhang Y., Yang H., Xu R., Huang G. - Overexpression of ZEB1 relates to metastasis and invasion in osteosarcoma. J. Surg Oncol 105:830-4; 2012.

Sheridan C., Kishimoto H., Fuchs R.K. et al. - CD44+/CD24- breast cancer cells exhibit enhanced invasive properties: an early step necessary for metastasis. Breast Cancer Res 8: R59; 2006.

Shibue T., Weinberg R.A. - EMT, CSCs, and drug resistance: The mechanistic link and clinical implications. Nat. Rev. Clin. Oncol., 14, 611–629; 2017.

Shin M.K., Cheong J.H. - Mitochondria-centric bioenergetic characteristics in cancer stem-like cells. Arch. Pharm. Res. 42, 113–127; 2019.

Siegel R.L., Miller K.D., Jemal A. - Cancer statistics. CA Cancer J Clin, 65: 5-29; 2015.

Siemann D.W. - The unique characteristics of tumor vasculature and preclinical evidence for its selective disruption by Tumor-Vascular Disrupting Agents. Cancer Treat. Rev. 37, 63–74; 2011.

Sies H. - Glutathione and its role in cellular functions. Free Radical Biology and Medicine 27: 916–921; 1999.

Sikalidis K.A. - Amino Acids and Immune Response: A Role for Cysteine, Glutamine, Phenylalanine, Tryptophan and Arginine in T-cell Function and Cancer? Pathology & Oncology Research 21, 9–17; 2015.

Smith M.A., Rubenstein L., Anderson J.R., Arthur D., Catalano P.J., Friedlin B. et al. - Secondary leukemia or myelodysplastic syndrome after treatment with intravenous epipodophyllotoxins. J. Clin Oncol 17:569–77; 1999.

Sontheimer H., Bridges R. - Sulfasalzine for brain cancer fits. Exp. Op. Invest. Drug 5: 575-578; 2012.

Sordet O., Khan Q.A., Pommier Y. - Apoptotic topoisomerase I-DNA complexes induced by oxygen radicals and mitochondrial dysfunction. Cell Cycle. 3(9):1095-7; 2004.

Spaderna S., Schmalhofer O., Wahlbuhl M. et al. - The transcriptional repressor ZEB1 promotes metastasis and loss of cell polarity in cancer. Cancer Res 68:537–44; 2008.

Spoelstra N.S., Manning N.G., Higashi Y., Darling D. et al. -The transcription factor ZEB1 is aberrantly expressed in aggressive uterine cancers. Cancer Res 66:3893-902; 2006.

Sreekumar R., Emaduddin M., Al-Saihati H., Moutasim K., Chan J.,. et al. - Protein kinase C inhibitors override ZEB1-induced chemoresistance in HCC. Cell Death Dis., 10, 703; 2019.

Su Y., Zhao B. et al. - Ferroptosis, a novel pharmacological mechanism of anti-cancer drugs. Cancer Lett., 483, 127–136; 2020.

Sun X., Rotenberg S.A. - Overexpression of Protein kinase Cα in MCF-10 human breast cancer cells engenders dramatic alterations in morphology, proliferation, and motility. Cell Growth Differ 10: 343-352; 1999.

Tam W.L., Lu H., Buikhuisen J., Soh B.S., Lim E. et al. - Protein kinase C is a central signaling node and therapeutic target for breast cancer stem cells. Cancer Cell, 24, 347–364. 79; 2013.

Tan S., L. Xia et al. - Exosomal miRNAs in tumor microenvironment, J. Exp. Clin. Cancer Res. 39 1–15; 2020.

Tao X., Wei D., Xiaoyu J. et al. – Molecular mechanisms of ferroptosis and its role in cancer Therapy. J. Cell Mol Med. 23:4900–4912; 2019.

Thiery J.P., Acloque H., Huang R.Y. et al. - Epithelial- mesenchymal transitions in development and disease. Cell, 139:871–90; 2009.

Toma J.G., McKenzie I.A., Bagli D., Miller F.D. - Isolation and characterization of multipotent skin-derived precursors from human skin. Stem Cells. 23: 727-37; 2005.

Townsend D. M., Tew Kenneth D. - The role of glutathione-S-transferase in anti-cancer drug resistance. Oncogene 22, 7369–7375; 2003.

Trachootham D., Alexandre J. and Huang P. - Targeting cancer cells by ROS-mediated mechanisms: a radical therapeutic approach? Nat Rev Drug Discov. 8(7): 579-91; 2009.

Trachootham D., Lu W., Ogasawara M.A., Nilsa R.D., Huang P. - Redox regulation of cell survival. Antioxid. Redox Signal. 10: 1343–1374; 2008.

Traverso N., Ricciarelli R., Nitti M., et al. - Role of glutathione in cancer progression and chemoresistance. Oxid. Med. Cell. Longev. 972913; 2013.

Uhr J.W., Pantel K. - Controversies in clinical cancer dormancy. Proc Natl Acad Sci USA. 108:12396 - 400; 2011.

Ursini F., Maiorino M. - Lipid peroxidation and ferroptosis: the role of GSH and GPx4. Free Radic. Biol. Med. 152, 175–185; 2020.

Ursini F., Maiorino M., Valente M., Ferri L., Gregolin C. - Purification from pig liver of a protein which protects liposomes and biomembranes from peroxidative degradation and exhibits glutathione peroxidase activity on phosphatidylcholine hydroperoxides. Biochim. Biophys. Acta 710, 197–211; 1982.

Valiente M. et al. - The evolving landscape of brain metastasis. Trends Cancer 4, 176–196; 2018.

Vazquez F., Lim J.H. et al. - PGC1α expression defines a subset of human melanoma tumors with increased mitochondrial capacity and resistance to oxidative stress. Cancer Cell, 23, 287–301; 2013.

Veal G.J., Errington J., Thomas H.D., Boddy A.W., Lowis S. - Biliary excretion of etoposide in children with cancer. Cancer Chemother Pharmacol 58:415–7; 2006.

Viale A., Pettazzoni P., Lyssiotis C.A., Giuliani V. et al. - Oncogene ablation-resistant pancreatic cancer cells depend on mitochondrial function. Nature, 514, 28–32; 2014.

Villablanca J.G., Volchenboum S.L. et al. - A Phase I New Approaches to Neuroblastoma Therapy Study of Buthionine Sulfoximine and MelphalanWith Autologous Stem Cells for Recurrent/Refractory High-Risk Neuroblastoma. Pediatr. Blood Cancer 63, 1349–1356; 2016.

Viswanathan V.S. et al. - Dependency of a therapy-resistant state of cancer cells on a lipid peroxidase pathway. Nature, 547, 453–457; 2017.

Vlashi E., Lagadec C., Vergnes L., Matsutani T., Masui K., Poulou M. et al. - Metabolic state of glioma stem cells and nontumorigenic cells. Proc Natl Acad Sci U S A. 108(38):16062–7; 2011.

Wada F., Koga H. - Highnexpression of CD44v9 and xCT in chemoresistant hepatocellular carcinoma: Potential targets by sulfasalazine. Cancer Sci. 109, 2801–2810; 2018.

Wahl C., Liptay S., Adler G., Schmid R.M. - Sulfasalazine: a potent and specific inhibitor of nuclear factor kappa B. J. Clin. Invest. 101: 1163-74; 1998.

Wang J.C. - Cellular roles of DNA topoisomerases: a molecular perspective. Nat Rev Mol Cell Biol 3:430–40; 2002.

Wang X., Zhang H., Chen X. - Drug resistance and combating drug resistance in cancer. Cancer Drug Resist 2:141–160; 2019.

Ways D.K., Kukoly C.A., de Vente J. et al. - MCF-7 breast cancer cells transfected with protein kinase C-α exhibit altered expression of other protein kinase C isoforms and display a more aggressive neoplastic phenotype. J. Clin. Invest. 95: 1906-1915; 1995.

Wei C.W., Yu Y.L. et al. - Anti-Cancer Effects of Sulfasalazine and Vitamin E Succinate in MDA-MB 231 Triple-Negative Breast Cancer Cells. Int. J. Med. Sci., 16, 494–500; 2019.

Williams D.A., Lemke T.L. - Foye's principi di chimicafarmaceutica. 924-950; 2005.

Xie Y., Hou W., Song X., Yu Y., Huang J., Sun X. et al. - Ferroptosis: process and function. Cell Death Differ. 23(3):369–79; 2016.

Yagoda N., Von R.M., Zaganjor E., Bauer A.J., Yang W.S., Fridman D.J. et al. - RASRAF- MEK-dependent oxidative cell death involving voltage-dependent anion channels. Nature 447:864–8; 2007.

Yamaguchi Y., Kasukabe T., Kumakura S. - Piperlongumine rapidly induces the death of human pancreatic cancer cells mainly through the induction of ferroptosis. Int J. Oncol. 52(3):1011–22; 2018.

Yan Y., Zuo X., Wei D. - Concise Review: Emerging Role of CD44 in Cancer Stem Cells: A Promising Biomarker and Therapeutic Target. Stem Cells Transl. Med. 4: 1033-1043; 2015.

Yan Y., Zuo X., Wei D. - Concise Review: Emerging Role of CD44 in Cancer Stem Cells: A Promising Biomarker and Therapeutic Target. Stem Cells Transl. Med. 4, 1033–1043; 2015.

Yang W. S. et al. - Regulation of ferroptotic cancer cell death by GPX4. Cell 156, 317–331; 2014.

Yang W.S. et al. - Peroxidation of polyunsaturated fatty acids by lipoxygenases drives ferroptosis. Proc. Natl. Acad. Sci. U. S. A. 113, E4966–E4975; 2016.

Yeldag G., Rice A., Del Rìo Hernandez A. - Chemoresistance and the self-maintaining tumor microenvironment. Cancer, 10 (12): E471; 2018.

Yin D., Chen K. - The essential mechanisms of aging: Irreparable damage accumulation of biochemical side-reactions. Exp Gerontol 40: 455-465; 2005.

Yoo S.E., Chen L., Na R. et al. - Gpx4 ablation in adult mice results in a lethal phenotype accompanied by neuronal loss in brain. Free Radic Biol Med. 52(9):1820-1827; 2012.

Yoshida G.J. - Emerging roles of Myc in stem cell biology and novel tumor therapies. J. Exp Clin Cancer Res. 37:173; 2018.

Yuan S., Norgard R.J., Stanger B.Z. - Cellular plasticity in cancer. Cancer Discov. 9:837–51; 2019.

Zhang Y., Tan H., et al. - Imidazole Ketone Erastin Induces Ferroptosis and Slows Tumor Growth in a Mouse Lymphoma Model. Cell Chem. Biol. 26, 623–633; 2019.

Zheng Z., Luo G. et al. - The Xc- inhibitor sulfasalazine improves the anti-cancer effect of pharmacological vitamin C in prostate cancer cells via a glutathione-dependent mechanism. Cell Oncol., 43, 95–106; 2020.

Zhou Y., Zhou Y., Shingu T., Feng L., Chen Z., Ogasawara M. et al. - Metabolic alterations in highly tumorigenic glioblastoma cells: preference for hypoxia and high dependency on glycolysis. J Biol Chem. 286(37):32843–53; 2011.

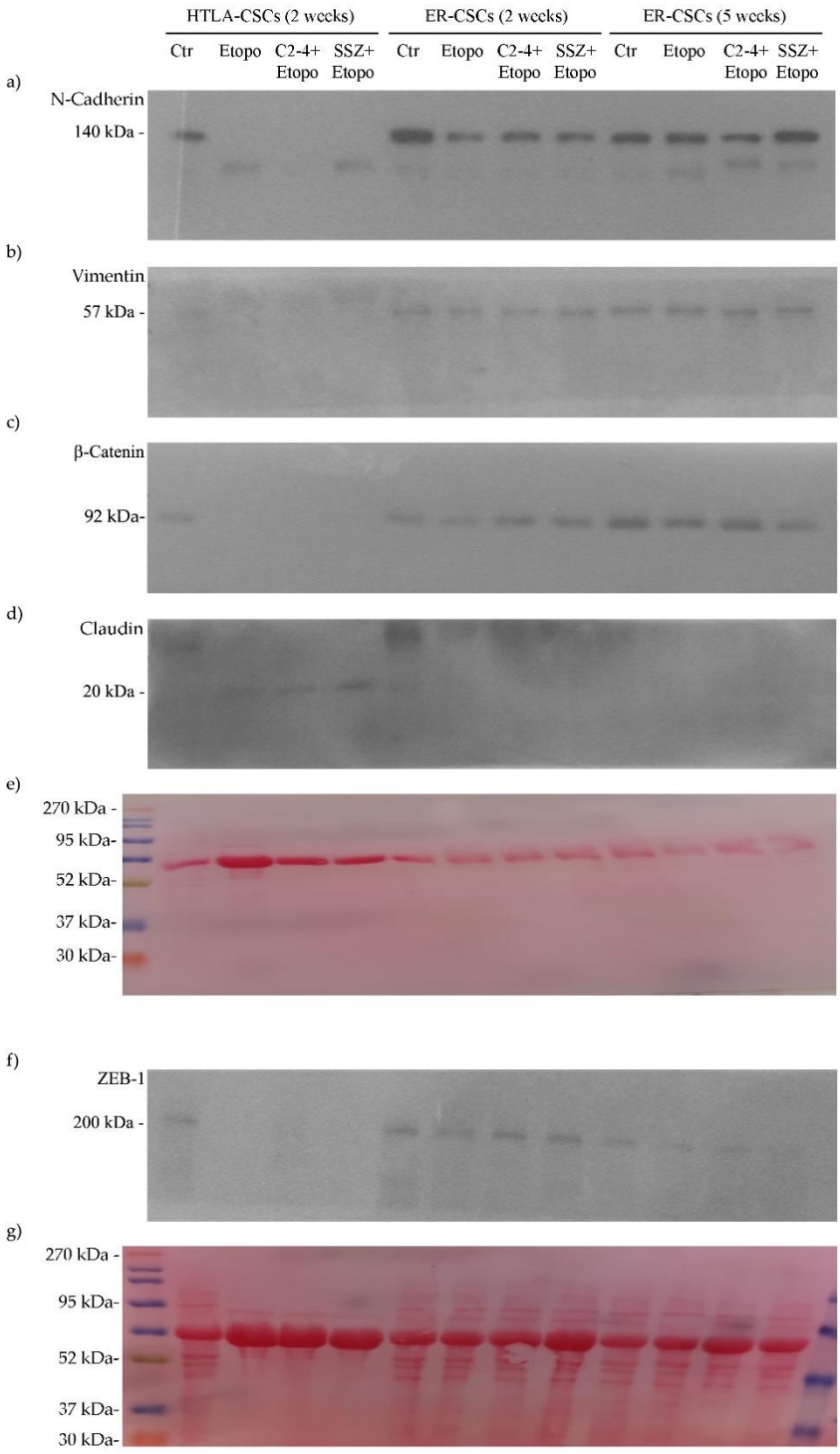

Supplementary material. Protein levels of N-Cadherin (a), Vimentin (b), β-Catenin (c), Claudin (d) and ZEB-1 (f) in both CSC populations treated for 2 or 5 weeks. Immunoblots shown are representative of three independent experiments. To ensure normalized protein content all filters were stained with Red Ponceau (e and g).